Taylor & Francis
Taylor & Francis Group

ORIGINAL RESEARCH

🔓 OPEN ACCESS

A novel regulation of PD-1 ligands on mesenchymal stromal cells through MMP-mediated proteolytic cleavage

Colette Dezutter-Dambuyant[a,b,c,d], Isabelle Durand[a,b,c,d], Laurent Alberti[a,b,c,d], Nathalie Bendriss-Vermare[a,b,c,d], Jenny Valladeau-Guilemond[a,b,c,d], Adeline Duc[a,b,c,d], Audrey Magron[a,b,c,d], Anne-Pierre Morel[a,b,c,d], Vanja Sisirak[a,b,c,d], Céline Rodriguez[a,b,c,d], David Cox[a,b,c,d], Daniel Olive[5,6], and Christophe Caux[a,b,c,d]

[a]Université de Lyon, Lyon, France; [b]Université Lyon 1, ISPB, Lyon, France; [c]INSERM U1052, Center de Recherche en Cancérologie de Lyon, Lyon, France; [d]CNRS UMR5286, Center de Recherche en Cancérologie de Lyon, Lyon, France; [5]Aix-Marseille Université, Marseille, France, Inserm U1068, Center de Recherche en Cancérologie de Marseille (CRCM), Immunity & Cancer Institut Paoli-Calmettes; [6]Aix-Marseille Université UM 105, CNRS UMR 7258, IBiSA Cancer Immunomonitoring Platform, Marseilles, France

ABSTRACT

Whether fibroblasts regulate immune response is a crucial issue in the modulation of inflammatory responses. Herein, we demonstrate that foreskin fibroblasts (FFs) potently inhibit $CD3^+$ T cell proliferation through a mechanism involving early apoptosis of activated T cells. Using blocking antibodies, we demonstrate that the inhibition of T cell proliferation occurs through cell-to-cell interactions implicating PD-1 receptor expressed on T cells and its ligands, PD-L1 and PD-L2, on fibroblasts. Dual PD-1 ligand neutralization is required to abrogate (i) binding of the PD-1-Fc fusion protein, (ii) early apoptosis of T cells, and (iii) inhibition of T cell proliferation. Of utmost importance, we provide the first evidence that PD-1 ligand expression is regulated through proteolytic cleavage by endogenous matrix metalloproteinases (MMPs) without transcriptional alteration during culture-time. Using (i) different purified enzymatic activities, (ii) MMP-specific inhibitors, and (iii) recombinant human MMP-9 and MMP-13, we demonstrated that in contrast to CD80/CD86, PD-L1 was selectively cleaved by MMP-13, while PD-L2 was sensitive to broader MMP activities. Their cleavage by exogenous MMP-9 and MMP-13 with loss of PD-1 binding domain resulted in the reversion of apoptotic signals on mitogen-activated $CD3^+$ T cells. We suggest that MMP-dependent cleavage of PD-1 ligands on fibroblasts may limit their immunosuppressive capacity and thus contribute to the exacerbation of inflammation in tissues. In contrast, carcinoma-associated fibroblasts appear PD-1 ligand-depleted through MMP activity that may impair physical deletion of exhausted defective memory T cells through apoptosis and facilitate their regulatory functions. These observations should be considered when using the powerful PD-1/PD-L1 blocking immunotherapies.

Abbreviations: ADAM,, A Disintegrin And Metalloproteinase; APC,, Antigen-Presenting Cell; APMA,, p-AminoPhenyl-Mercuric Acetate; BM-MSC,, Bone Marrow-derived Mesenchymal Stem Cell; CFSE,, CarboxyFluorescein Succinimidyl Ester; CLSPA,, Chromatographically purified collagenase; DC,, Dendritic Cell; ddPCR,, droplet digital PCR; ECM,, Extra-Cellular Matrix; EGFR,, Epidermal Growth Factor Receptor; FCS,, Foetal Calf Serum; FF,, infant Foreskin Fibroblasts; Gy,, Gray; IFNγ,, interferon gamma; IL-10,, InterLeukin-10; IL-17A,, InterLeukin-17 A; IL-1α,, InterLeukin-1 α; IL-6R,, InterLeukin-6 Receptor; mAb,, monoclonal Antibody; MDC,, myeloid Dendritic Cell; MFI,, Mean Fluorescence Intensity; MMP,, Matrix MetalloProteinase; Mo-DC,, Monocyte-derived dendritic cell; MSC,, Mesenchymal Stem Cell; NK,, natural killer; PBS,, Phosphate-Buffered Saline; PD-1,, Programmed cell Death protein-1; PD-L1,, Programmed Death-Ligand 1; PD-L2,, Programmed Death-Ligand 2; PFA,, ParaFormAldehyde; PHA,, PhytoHemAglutinin; PI,, Proliferation Index; PS,, PhosphatidylSerine; rh,, recombinant human; SA-β-gal,, senescence-associated β-galactosidase; sPD-L1,, soluble PD-L1 form; TGFβ,, Transforming Growth Factor β; TNFα,, Tumor Necrosis Factor α; γ-FF,, 30 Gray-irradiated infant Foreskin Fibroblast; γ-irradiation,, 30-Gray irradiation

Introduction

Stromal cells such as fibroblasts are traditionally viewed as constituents of connective tissues, passively providing structural and homeostatic support. Fibroblasts are mainly involved in the synthesis of extracellular matrix (ECM) and in the definition of the structure of tissue environment. Furthermore, it becomes evident that fibroblasts may also shape innate and adaptive immune responses involved in host defense, tumor immunity, and autoimmunity.[1-3] Fibroblasts isolated from different anatomic sites have distinct transcriptional patterns and exhibit different functional properties[4] such as migrating ability, ECM production and degradation, and contractility. More recently, their active role in the control of inflammatory response has been reported.[1-3]

The immunosuppressive effects of mesenchymal stem cells (MSCs) is a fundamental property.[1,3] shared by adult dermal

fibroblasts[5] and mature mesenchymal stromal cells.[6,7] Within an immune reaction, stromal cells modulate immune cell behavior by conditioning the local cellular and cytokine milieu. Fibroblasts control the accumulation, retention, survival, activation, and differentiation of immune cells in a site-dependent manner at sites of inflammation. This control is achieved through cellular cross-talk with immune cells and through their production of cytokines (IL-1, TGFβ, IL-6, and IL-8), chemokines (CCL2 or MCP-1, CXCL1 or Groα, and CXCL10 or IP-10), enzymes (indoleamine 2,3-dioxygenase, prostaglandin-endoperoxide synthase 2), prostaglandin E2, and adhesion molecules.[8] Fibroblasts derived from sites of chronic inflammation such as inflamed synovial joints in rheumatoid arthritis patients possess an imprinted phenotype that is stable in long-term culture. Fibroblasts modify the quality and the quantity of the inflammatory infiltrate during the induction of inflammatory response and influence the switch from acute to chronic inflammation.[9,10]

At the termination of response, fibroblasts contribute to the resolution of inflammation by withdrawing survival signals and normalizing the chemokine gradients, thereby constraining infiltrating leukocytes to undergo apoptosis or leave the tissue through draining lymphatics.[9] Most previous studies have reported the effects of fibroblasts on lymphocytes in non-malignant[5-7] and malignant tissues[11] through production of cytokines, chemokines, biologically active factors, and chemical mediators.[8] Herein, we have focused our interest on the immunomodulatory cross-talk between membrane-associated molecules (e.g. Programmed Death Ligand-1, B7-H1/PD-L1, and Programmed Death Ligand-2, B7-DC/PD-L2) expressed on fibroblasts and their receptor PD-1 expressed on T cells. PD-1 expression is induced when T cells become activated,[12] as well as during T cell differentiation toward effector cells.[13] PD-1 is expressed on activated T cells including immunosuppressive CD4+ T cells (TReg) and exhausted CD8+ T cells, but also on B cells, myeloid dendritic cells (MDCs), monocytes, thymocytes, and natural killer (NK) cells. This broad PD-1 expression suggests a wide implication of the PD-1 pathway needed for effective immunity and maintenance of T cell homeostasis.[14] Within the tumor microenvironment, PD-1 is highly expressed on a large proportion of tumor-infiltrating lymphocytes from many different tumor types and suppresses local effector immune responses. Indeed, blockade of the PD-1 pathway was shown to enhance antitumor immune response.[15] As the expression of PD-L1/-L2 in the tumor environment represents a major immune escape mechanism, therapy blocking PD-1 has very recently shown unprecedented rates of durable clinical response in a variety of cancer types.[16-19] Of relevance, high levels of PD-L1 expression in the tumor microenvironment appear predictive of a better clinical response to therapies targeting the PD-1/PD-L1 pathway.[17,20-22] In addition to its expression on tumor cells, PD-L1 is also expressed on B cells, DCs, macrophages and T cells, and is upregulated after their activation. PD-L1 is also detected on several non-hematopoietic cell types including lymphatic and micro-vascular endothelial cells,[23,24] pancreatic islet cells,[25] and keratinocytes in particular upon cytokine exposure.[26] The expression of PD-L2 was initially thought to be restricted to antigen-presenting cells (APCs) such as macrophages and DCs.[27] However, PD-L2 expression can be induced on a wide variety of other immune cells and non-immune cells depending on environmental stimuli.[12] As PD-L2 is generally expressed at lower level, PD-L1 is still considered the more dominant negative inhibitory molecule.[28] although relative PD-L1/PD-1 affinity is lower than PD-L2/PD-1.[29] MSCs, normal fibroblasts, human colonic fibroblasts in gut mucosa, and also non-small-cell lung tumor-associated fibroblasts constitutively express PD-L1 and PD-L2.[11,30-33] Although PD-1 ligand expression on stromal cells is relatively well known, their function in immune regulation remain largely elusive either in a chronic inflammatory context or in a tumor microenvironment.

Herein, we focused our interest on a population of dermal fibroblasts, the infant FFs. We provide evidence that, upon culture, FFs express PD-L1 and PD-L2 which are upregulated in vitro by pro-inflammatory cytokines. We also report that similarly to murine[30] and human[34] MSCs, FFs suppress activated CD3+ T cell proliferation. This inhibitory effect was due to the induction of early apoptotic signals on mitogen-activated T cells through a cell-to-cell contact involving PD-1 inhibitory molecule on T cells and its ligands PD-L1 and PD-L2 on FFs. More importantly, and for the first time to our knowledge, we demonstrate that MMPs, mainly MMP-13, modulate the expression of both PD-1 ligands through the cleavage of their PD-1 binding domain. Taken together, these novel data suggest that PD-1 ligands expressed by fibroblasts are among the critical processes that suppress T cell response in inflamed or diseased tissues. Furthermore, disruption of this pathway by MMPs might lead to exacerbated inflammation associated with severe tissue damage and/or impaired physical deletion of exhausted defective memory T cells through apoptosis by driving the increase of the magnitude of T cell response.

Results

Both irradiated and non-irradiated infant foreskin fibroblasts express PD-1 ligands able to interact with the soluble PD-1-Fc fusion protein

Our study was performed with 30 Gray-irradiated infant foreskin fibroblasts (γ-FFs) instead of non-irradiated FFs in order to strictly abrogate fibroblast proliferation without affecting their immunosuppressive capacity, as reported on bone marrow-derived mesenchymal stem cells (BM-MSCs).[35,36] Flow cytometry analysis showed that γ-FFs retain similar phenotype compared to non-irradiated cells: (i) expression of mesenchymal markers (CD73, CD90, and CD105), (ii) lack of hematopoietic and co-stimulatory molecules (CD45, CD80, and CD86), (iii) lack of other lineage markers (CD34, MASC-1, and low CD146) (Fig. S1A), and (iv) constant expression of MHC class I molecules (HLA-A, B, C) and absence of MHC class II (HLA-DR) molecules (Fig. 1A). Like non-irradiated FFs, γ-FFs respond to pro-inflammatory cytokines with strong upregulation and induction of MHC class I and MHC class II (HLA-DR) expression respectively in response to IFNγ and low MHC class I upregulation in response to TNFα, while CD80 and CD86 were not induced (Fig. S1B). These results showed that γ-FFs behave like non-irradiated FFs.
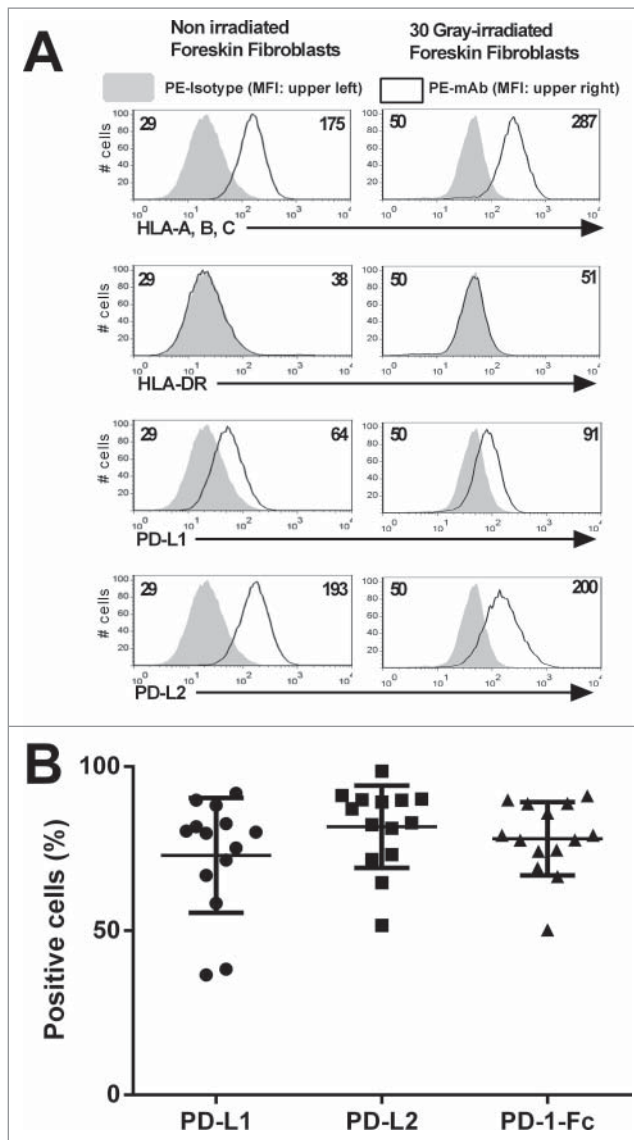
Figure 1. Infant foreskin fibroblasts express PD-L1 and PD-L2 molecules and bind PD-1-Fc fusion protein. (A) PD-L1 and PD-L2 expression on infant foreskin fibroblasts (FFs) is not modulated by a 30 Gray-irradiation after 3–5 passages. The expression of surface markers was analyzed by flow cytometry on FFs that were irradiated or not and cultured for 48 h under an identical seeding concentration. Flow histograms are representative of n = 3 independent experiments. Filled histograms showed isotype control staining and open histograms showed the specific expression of the indicated cell surface marker. Mean Fluorescence Intensity (MFI) values are indicated upper left for isotype mAb and upper right for specific markers. (B) Frequency of PD-L1 and PD-L2 expression, and of PD-1-Fc fusion protein binding on 30 Gray-irradiated infant foreskin fibroblasts. The frequency of cells expressing PD-L1, PD-L2, and binding PD-1-Fc fusion protein was analyzed by flow cytometry on γ-FFs after 24 h of culture under an identical seeding concentration. Each symbol represents a different FF donor, n = 14 independent donors are shown.

Importantly, we showed that FFs expressed significant levels of PD-L1 and PD-L2 that were not modulated upon γ-irradiation (Fig. 1A). As a first evaluation of the relevance of PD-L1 and PD-L2 expression on γ-FFs, we investigated the binding of soluble PD-1-Fc fusion protein. Among 14 different γ-FFs, the frequency of PD-1-Fc$^+$ γ-FFs ranges from 66.3 to 83.4% (78.1 $\pm$ 11.3%) and the percentages of γ-FFs expressing PD-L1 (72.9 $\pm$ 17.5%) and PD-L2 (81.7 $\pm$ 12.5%) were similar. (Fig. 1B)

The PD-1-Fc binding on γ-FFs (Fig. 2A–E) was marginally affected by pre-incubation with anti-PD-L1 monoclonal antibody (mAb) (less than 9.5% inhibition whatever the concentration of mAbs used (Fig. 2B–E) and massively abrogated by pre-incubation with anti-PD-L2 mAb (more than 89.6% inhibition whatever the concentration of mAbs used (Fig. 2C–E) and totally abrogated by pre-incubation with both anti-PD-L1 (50 μg/mL) and anti-PD-L2 (10 to 50 μg/mL) mAbs (less than 1% of positive γ-FFs e.g., more than 98.7% inhibition (Fig. 2D–E). Pre-incubation with mixed IgG$_{2a}$ (50 μg/mL)/IgG$_{2b}$ (10 to 50 μg/mL) isotype-matched controls did not change the PD-1-Fc binding on γ-FFs (Fig. 2E). The same observation was made when analyzed in mean fluorescence intensity (MFI) (Fig. 2F). This abrogation was still complete with very low concentrations of PD-L2 mAb (40 ng/mL) and 50 μg/mL PD-L1 mAb (data not shown). Similar profiles of mAb-dependent blockade of PD-1-Fc binding were obtained when γ-FFs were harvested either through an enzymatic cell dissociation buffer (trypsin/EDTA) or through an EDTA-based chelating agent (Versene^{TM}) (Fig. S2). Although anti-PD-L2 mAb is indeed the dominant blocking mAb, both anti-PD-L1 and anti-PD-L2 mAbs were required to reach a complete blockade of PD-1-Fc binding.

Non-irradiated FFs and γ-FFs shared a similar surface marker profile, and expressed PD-L1 and PD-L2 retaining the capacity to bind a soluble PD-1-Fc fusion protein. The abrogation of the binding to PD-1-Fc fusion protein required additive blockade by anti-PD-L1 and anti-PD-L2 mAbs.

Pro-inflammatory cytokines upregulate the expression of PD-1 ligands on infant foreskin fibroblasts

We next showed that PD-L1 expression was specifically upregulated in response to IFNγ (Fig. 3, Fig. S3 and S4), while PD-L2 expression levels were increased by IFNγ, TNFα, IL-1α, and TGFβ resulting in potent increase in PD-1-Fc binding in response to most pro-inflammatory cytokines (Fig. 3B and Fig. S3B). The addition of IFNγ to TNFα and IL-1α did not favor a greater increase in PD-L2 expression (Fig. S4A), but resulted in a greater increase in PD-1-Fc binding (Fig. S4B). γ-FFs retained the ability to respond to pro-inflammatory cytokines and consequently, to increase the PD-1-ligand interactions to the soluble PD-1-Fc fusion protein. PD-L1 expression was enhanced only by IFNγ while PD-L2 expression was more slightly enhanced by other cytokines.

γ-irradiated infant foreskin fibroblasts suppress mitogen-activated T-cell proliferation through early apoptosis

The effect of γ-FFs on CD3$^+$ T cell proliferation and activation in presence of the mitogen PHA was examined, as previously reported.[6] The γ-FFs were plated at three different densities and cultured for 24 h/48 h before successive additions of Carboxyfluorescein succinimidyl ester (CFSE)-stained T cells and of the mitogen PHA. We observed that γ-FFs inhibited PHA-stimulated CD4$^+$ and CD8$^+$ T cell proliferation in a dose-dependent manner (Fig. 4A1–2). The suppression was potent as the inhibitory effects were already significant at a ratio of
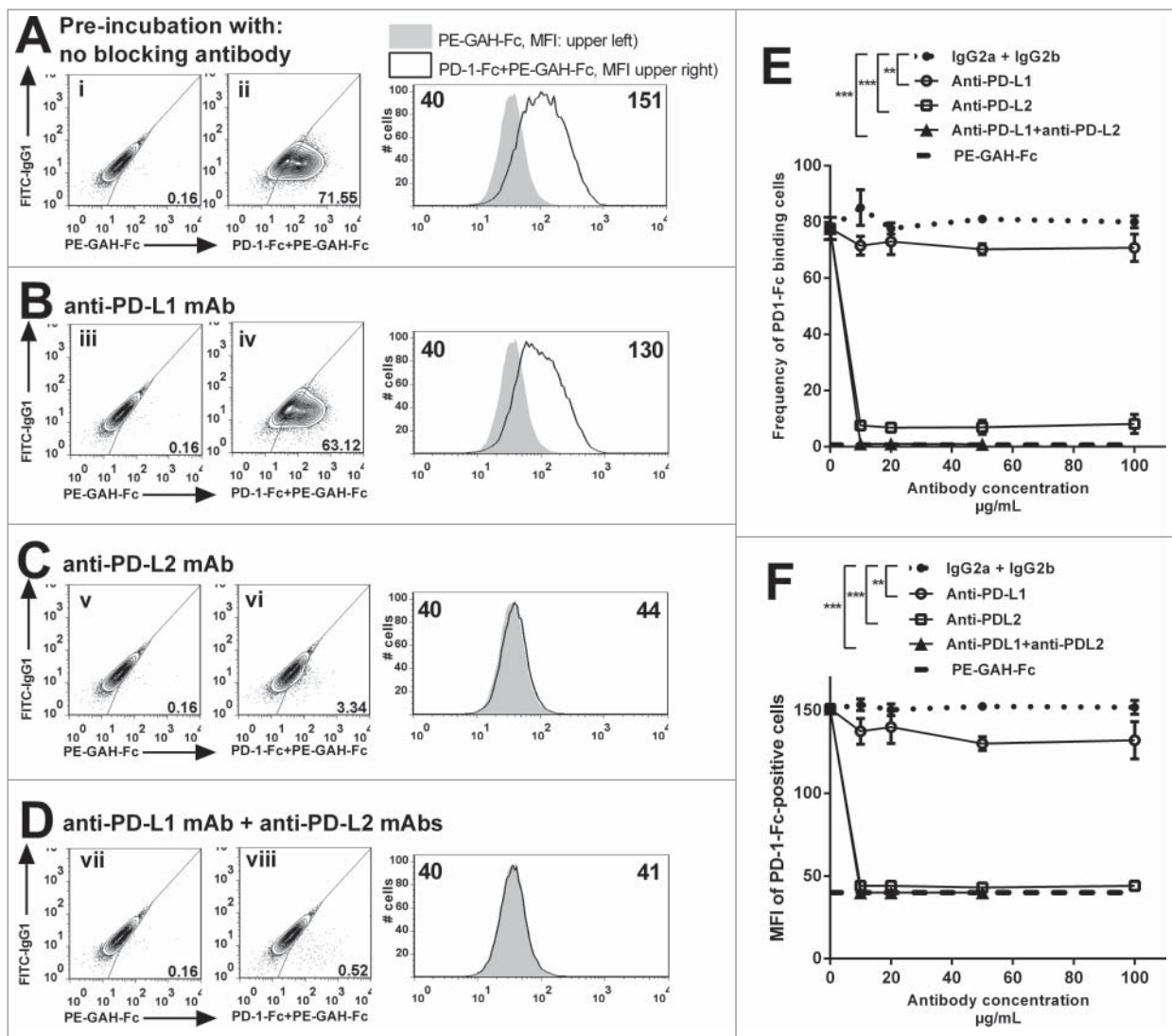
Figure 2. Binding of PD-1-Fc fusion protein on 30 Gray-irradiated infant foreskin fibroblasts is abrogated by anti-PD-1 ligand mAbs. The binding of PD-1-Fc fusion protein (PD-1-Fc) to γ-FFs was analyzed before (i and ii) and after (from iii to viii) exposure to blocking anti-PD-L1 (clone 29E2A3) and/or anti-PD-L2 mAbs (clone 24F10C12). Representative dot plots showing isotype control (i, iii, v, and vii) and PD-1-Fc binding (ii, iv, vi, and viii) on γ-FFs non pre-incubated (A) or pre-incubated with PD-L1 (B), PD-L2 (C), and both PD-L1 and PD-L2 (D) blocking mAbs. (A–D) Representative flow histogram overlay of PE-GAH-Fc control (filled histograms) and of PD-1-Fc + PE-GAH-Fc (open histograms). Mean Fluorescence Intensity (MFI) values are indicated upper left for negative control and upper right for PD-1-Fc. (E) Frequency and (F) MFI of positive cells showing binding to PD-1-Fc fusion protein. PD-1-Fc binding was neutralized by anti-PD-L1 (open circle), anti-PD-L2 alone (open square) or combined to 50 μg/mL anti-PD-L1 (closed triangle) blocking mAbs at the indicated concentrations. Closed circle on dotted lines represent isotype-matched controls (mixed IgG$_{2a}$ (50μg/mL)/IgG$_{2b}$) and large dotted lines represent PE-conjugated goat anti-human immunoglobulin Fc portion (PE-GAH-Fc) alone. Data are representative of n = 3 independent experiments (n = 2 γ-FF donors). Bars represent the SD. $^{**}p < 0.01$ and $^{***}p < 0.001$.

1.25 γ-FFs to 100 T cells and more visible on the CD4$^+$ T cells (77.9 $\pm$ 2.6% inhibition) than CD8$^+$ T cells (56.1 $\pm$ 3.7% inhibition).

Next, we pre-incubated γ-FFs in presence of pro-inflammatory cytokine cocktails (TNFα + IL-1α or IFNγ + TNFα + IL-1α) to increase PD-1 ligand expression (Fig. S4). Cytokine pre-stimulation of γ-FFs did not lead to a significant increase in the γ-FFs-mediated suppression of activated CD4$^+$ T cell proliferation and activated CD8$^+$ T cell proliferation (except for the TNFα + IL-1α + IFNγ cocktail), in a ratio-dependent manner (Fig. 4A1–2). At a ratio of 2.5 γ-FFs pretreated with TNFα/IL-1α to 100 T cells, the percent inhibition was 71.4$\pm$4.0% and 53.5$\pm$1.0% for CD4$^+$ and CD8$^+$ T cells, respectively. At a similar γ-FF:T cell ratio, when γ-FFs were pretreated with TNFα + IL-1α + IFNγ, the CD4$^+$ T cells and the CD8$^+$ T cells were similarly suppressed with 75.7 $\pm$ 2.3% and 74.7 $\pm$ 5.9%

inhibition, respectively (Fig. 4A1–2). Although γ-FF pretreatment with cytokine cocktails leads to a high increase of PD-1 ligand expression (Fig. S4), upregulation of MHC molecules may also be induced (Fig. S1) and other soluble mediators may be released (data not shown) which may partly compensate for the increase of PD-1 engagement.

To determine the mechanism by which γ-FFs suppressed both activation and proliferation of T cells cultured in presence of PHA, in CD4$^+$ and CD8$^+$ T cell subsets we compared: (i) the absolute cell numbers, (ii) the percentage of dividing cells, and (iii) the Proliferation Index (PI) of the proliferative response assessed by CFSE dilution. We compared culture conditions in absence of γ-FFs or in presence of non-treated and treated γ-FFs by TNFα + IL-1α +/$-$ IFNγ. At a ratio 5 γ-FF:100 T cells (Fig. 4B1–2), we observed a decrease of 32–34% of the PI for the CD4$^+$ T cells and the CD8$^+$ T cells,
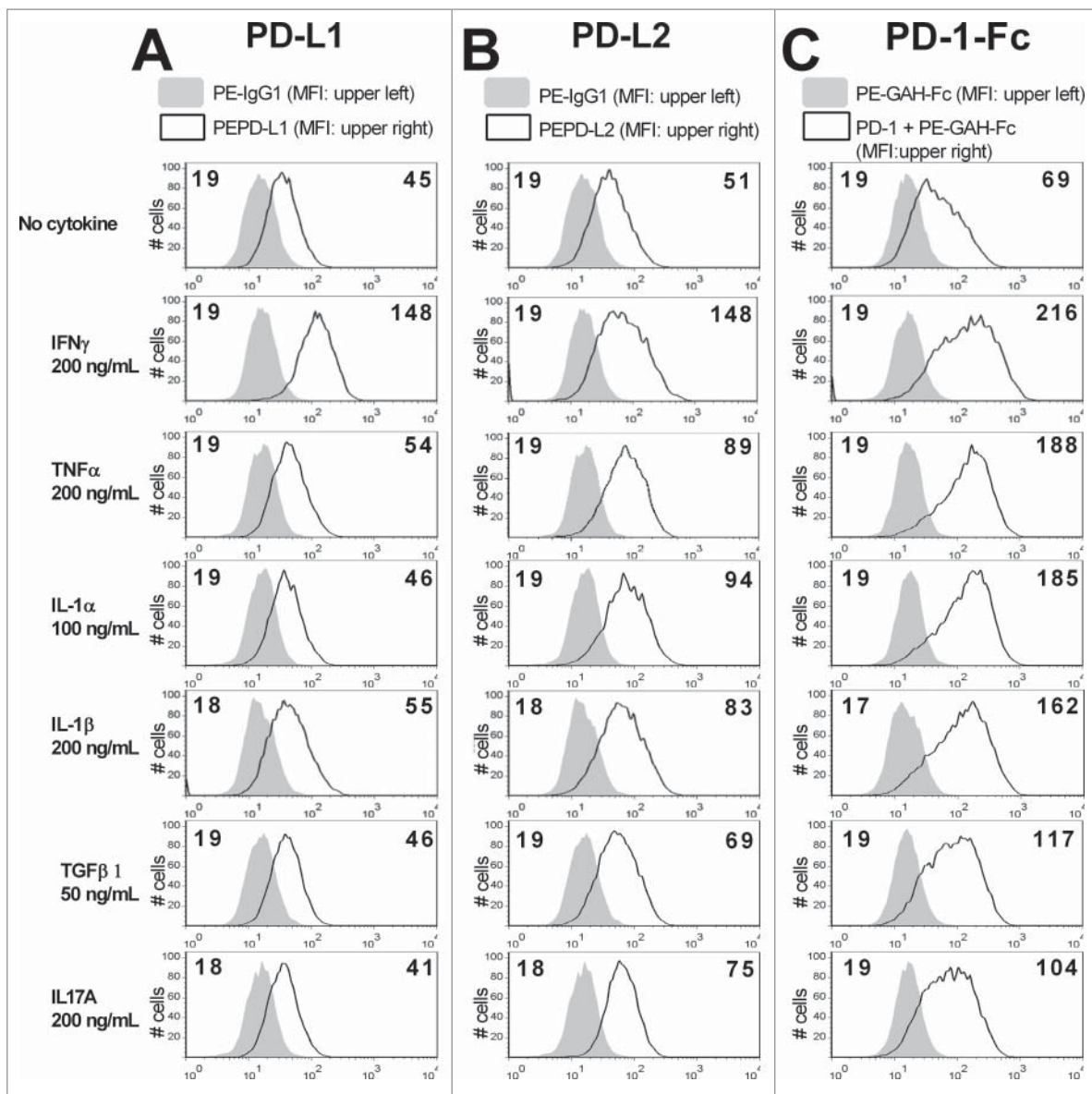
Figure 3. At low seeding density, 30 Gray-irradiated infant foreskin fibroblasts upregulate PD-1 ligand expression and their capacity to bind PD1-Fc fusion protein in presence of pro-inflammatory cytokines. γ-FFs seeded at $7 \times 10^3/\text{cm}^2$ were maintained in culture for 2 d in presence of pro-inflammatory cytokines (IFNγ, TNFα, IL-1α, IL-1β, TGFβ1, and IL-17A). Expression levels of PD-1 ligands and binding capacity of PD-1-Fc were detected by flow cytometry. (A, B) Representative flow histogram overlay showing isotype control staining (filled histograms) and specific expression of PD-L1 and PD-L2 (open histograms). Mean Fluorescence Intensity (MFI) values are indicated upper left for isotype mAb and upper right for specific markers. (C) Representative flow histogram overlay showing control staining with PE-GAH-Fc (filled histograms) with MFI value in upper left and PD-1-Fc binding (open histograms) with MFI value in upper right. Cytometry data are representative of n = 3 independent experiments.

respectively. A similar distribution of the CFSE profile for every T cell subpopulation whatever the pre-treatment of γ-FFs by TNFα + IL-1α +/− IFNγ suggest identical number of T cell division for CD4$^+$ T cells and for CD8$^+$ T cells, respectively. In contrast, we observed an important reduction of the absolute numbers of CD4$^+$ T cells and CD8$^+$ T cells in presence of γ-FFs. Fig. 4A1–2 showed summary data at the three different γ-FFs to target CD3$^+$ T cell ratios. These results suggest that γ-FFs suppressed T cell proliferation by limiting the number of T cells initially entering in division and that the non-dividing T cells are lost. One hypothesis is that the immunosuppression of γ-FFs occurred at a very early step of T cell proliferation by increasing early apoptosis and limiting the number of T cells retaining the ability to achieve proliferation in response to the mitogen.

We then examined whether γ-FFs triggered apoptosis of short time PHA-activated T cells. The percentage of early apoptotic T cells was assessed (DAPI-/Annexin V$^+$ CD3$^+$ T cells) after 3 h of co-culture without PHA addition and 17 h of co-culture in presence of PHA (20 h) (Fig. S5). In presence of γ-FFs, a strong increase of apoptosis ($p < 0$ .05) was observed (Fig. 4C) at 20 h including 17 h of PHA activation. In the CD4$^+$ T cell subset, 58.8±5.2% of cells were DAPI$^-$/Annexin V$^+$ with γ-FFs *versus* 27.6±8.0% without γ-FFs. In the CD8$^+$ T cell subset, 66.3±7.4% of cells were DAPI$^-$/Annexin V$^+$ with γ-FFs *vs.* 33.9±9.0% without γ-FFs. Similar results were observed after a pre-incubation of γ-FFs with TNFα (100 ng/mL) that was chosen in order to selectively favor the upregulation of PD-L2 and PD-1 binding and not that of PD-L1 (Fig. 4C). These data confirmed that γ-FFs limited the number
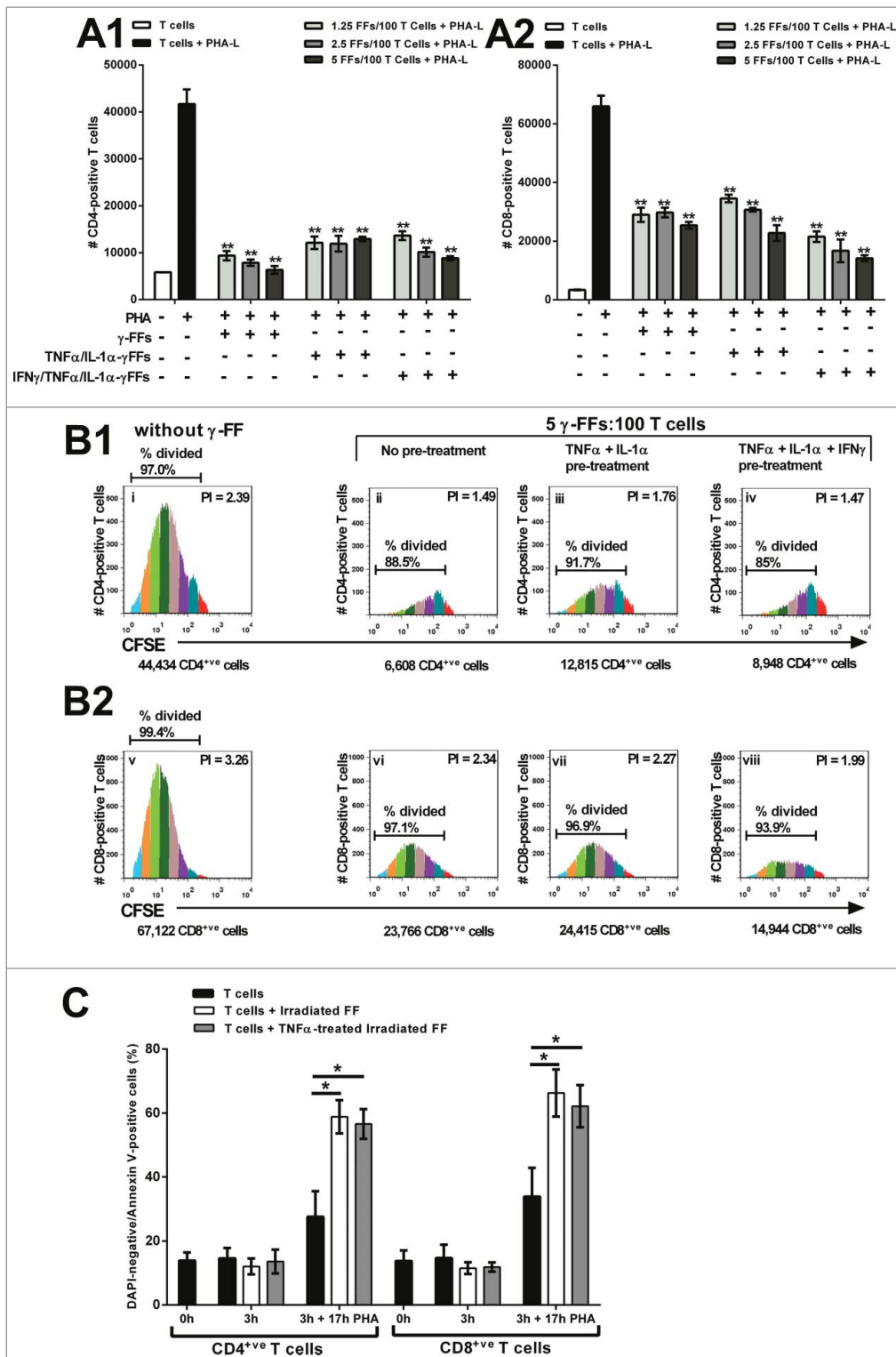
Figure 4. 30 Gray-irradiated infant foreskin fibroblasts reduce the numbers of mitogen-activated CD3$^+$ cells upon co-culture by inducing early apoptosis of PHA-activated T cells. The proliferative response of CFSE-labeled CD3$^+$ T cells, co-labeled with anti-CD4$^+$ and anti-CD8$^+$ antibodies was analyzed by flow cytometry after 7 d of co-culture on plated γ-FFs, and activation by PHA-L (0.5μg/mL). (A1, A2) Data showed the number of CD4$^+$ and CD8$^+$ T cells among total CD3$^+$ T cells (calculated on FlowJo$^®$ software) cultured for 5 d on γ-FFs at different ratios of 1.25 γ-FFs:100 T cells, 2.5 γ-FFs:100 T cells and 5 γ-FFs/100 T cells (n = 3 independent experiments). Significant value is $^{**}p < 0.01$ between "T cells+PHA-L" (black histogram) and all other conditions (multiple gray histograms). (B1, B2) Representative FlowJo$^®$ analysis of the CFSE dilution (PI: Proliferation Index), the numbers of CD4$^+$ and CD8$^+$ T cells, and the percentage of divided CD4$^+$ (i–iv) and CD8$^+$ T cells (v–viii) at a ratio of 5 γ-FFs: 100 CD3$^+$ T cells. (C) The percentage of early apoptotic CD3$^+$ T cells (DAPI$^-$/Annexin V$^+$ T cells) was determined in absence or in presence of γ-FFs treated or not by TNFα at a ratio of 5 γ-FFs:100 T cells. Before co-culture with γ-FFs (0 h), after 3 h of co-culture with γ-FFs (3 h), and after 3 h of co-culture with γ-FFs and then 17 h of PHA (0.25 μg/mL) activation (3 h + 17 h PHA), T cells were co-labeled with anti-CD4 PerCP-Cy5.5-mAb and anti-CD8 APC-mAb, stained with PE-Annexin V, and then analyzed by flow cytometry. Summation data of six independent experiments are shown (n = 4 T cell donors and n = 2 γ-FF donors). Bars represent the SD. $^*p < 0.05$.

of T cells capable of proliferation by increasing T cell apoptosis at a very early stage of T cell proliferation.

PD-L1 and PD-L2 blockade on γ-irradiated FFs reverts the inhibition of T cell proliferation and the induction of T cell apoptosis

Previous functional studies reported that PD-L1 and PD-L2 exert overlapping effects on T cell response.[37] To assess the functional significance of the expression of PD-1 ligands on γ-FFs, we examined the impact of anti-PD-L1 and anti-PD-L2 neutralizing mAbs in γ-FFs-mediated suppression of PHA-stimulated CD3$^+$ T cell proliferation. A pre-incubation of γ-FFs with both blocking anti-PD-1 ligand mAbs but not isotype controls, partially restored PHA-stimulated CD4$^+$ T cell numbers, but increased rescue was observed in presence of

TNFα-treated γ-FFs expressing more PD-L2 ($p < .01$ at both ratios) (Fig. 5A1–2). Of importance, the restoration was complete in the CD8$^+$ T cell subset, even more strikingly when co-cultured with TNFα-treated γ-FFs. Following PD-1 ligand blockade, the functional influence of the diverse array of small molecules secreted by TNFα-treated γ-FFs (growth factors, chimiokines, and cytokines) and direct cell–cell contact might promote specific CD8$^+$ T cell proliferation. Collectively, these data demonstrate that γ-FFs-mediated suppression of PHA-stimulated CD3 T cell proliferation involved PD-1 ligands.

We then analyzed the consequences of PD-1 ligand blockade on γ-FFs-induced apoptosis of PHA-activated CD3$^+$ T cells (Fig. 5B1–2). Neutralization with mixed anti-PD-L1 and anti-PD-L2 mAbs, but not isotype-matched controls, significantly reduced the percentage of early apoptotic T cells triggered by γ-FFs. Indeed, the γ-FFs induced apoptosis decreased from
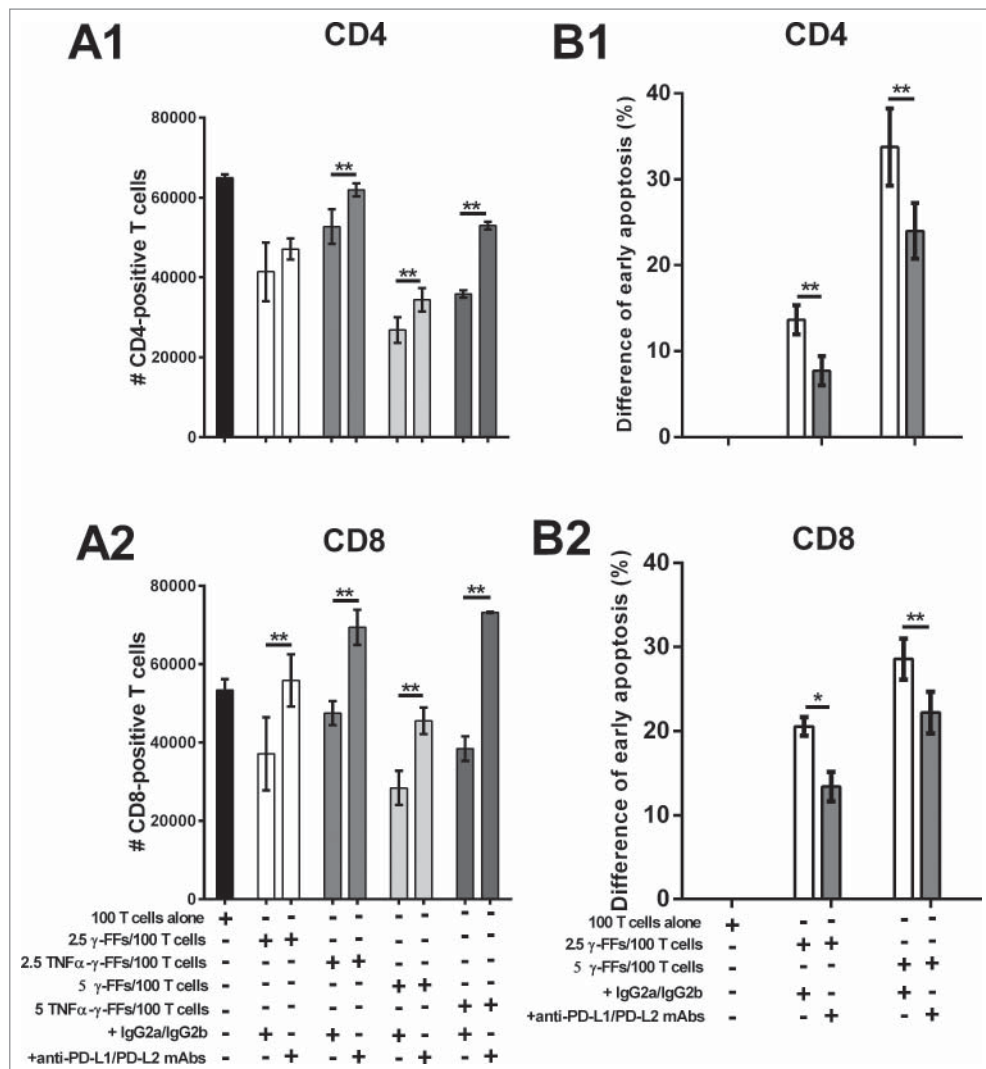

Figure 5. PD-L1 and PD-L2 blockade by mAbs reverts the inhibition of T cell proliferation and the induction of T cell apoptosis triggered by 30 Gray-irradiated infant foreskin fibroblasts. (A1, A2) PHA was added to a co-culture of γ-FFs pre-treated or not with TNFα and CD3$^+$ T cells at different ratios of 2.5 γ-FFs:100 T cells and 5 γ-FFs:100 T cells. Flow cytometry analysis of the number of the total bulk CD3$^+$ T cells, co-labeled with anti-CD4 and anti-CD8 mAbs was performed after 7 d of co-culture in the presence or not of anti-PD-L1 (clone 29E23A3)/anti-PD-L2 (clone 24F10C12) mAbs or isotype control antibodies (mouse IgG$_{2a}$/IgG$_{2b}$). Results are mean $\pm$ SD of the number of CD4$^+$ cells and CD8$^+$ T cells within the CD3$^+$ T cells and are representative of three independent experiments. Bars represent the SD, $^{**}p < 0.01$. (B1, B2) The blocking capacity of mixed anti-PD-L1 (clone 29E23A3) and anti-PD-L2 mAbs (clone 24F10C12), compared to mixed isotype controls (mouse IgG$_{2a}$/IgG$_{2b}$) was determined by the difference of percentage of early apoptotic CD3$^+$ T cells (DAPI$^-$/Annexin V$^+$ T cells) in presence or in absence of γ-FFs at two ratios of 2.5 γ-FFs:100 T cells and 5 γ-FFs:100 T cells. 17 h after PHA stimulation in the conditions as indicated, T cells were co-labeled with anti-CD4-FITC mAb and anti-CD8-PerCP-Cy5.5 mAb, stained with PE-Annexin V, and then analyzed by flow cytometry. Results are representative of n = 3 independent experiments. Bars represent the SD. $^*p < 0.05$, $^{**}p < 0.01$.

13.7±1.7% to 8.1±1.6%, $p < 0.01$ (2.5 γ-FF:100 T cell ratio) and from 33.8±4.5% to 24.0±3.3%, $p < 0.01$ (5 γ-FF:100 T cell ratio) in the CD4$^+$ T cell subset. In the CD8$^+$ T cell subset, γ-FFs induced apoptosis decreased from 20.6±1.1% to 13.4± 1.8%, $p < 0.05$ (2.5 γ-FF:100 T cell ratio) and from 28.6±2.4% to 22.2±2.5%, $p < 0.01$ (5 γ-FF:100 T cell ratio) (Fig. 5B1–2). These experiments confirm that both PD-L1 and PD-L2 expressed on γ-FFs play a role in the induction of early apoptosis of PHA-activated T cells co-cultured with γ-FFs.

PD-1 ligand expression is lost on γ-irradiated infant foreskin fibroblasts as a function of time and cell-seeding density

By contact-inhibition, primary fibroblasts can be induced into reversible quiescence, but unlike most primary cells, fibroblasts remain healthy and highly active metabolically in culture in a quiescent state for as long as 30 d with little apoptosis or senescence.[38,39] We investigated the impact of cell density and culture time on PD-1 ligand and CD10 expression. CD10 was chosen as a reference surface molecule on γ-FFs. γ-FFs were cultured at the seeding cell concentration of 13 × 10^3/cm^2 and analyzed for PD-L1 and PD-L2 expression and PD-1-Fc binding by flow cytometry (frequency and MFI) on day 1, day 4, and day 14 of culture. A progressive loss of PD-L1 and PD-L2 expression and PD-1-Fc binding (both percentages (Fig. 6B) and relative MFI values (Fig. 6C) was observed from day 1 up to day 14 on DAPI$^-$ adherent fibroblasts. The loss for PD-L1 expression level (loss of 63.8% PD-L1$^+$ cells and of 54.2% MFI ratio), that of PD-L2 (loss of 64.7% PD-L2$^+$ cells and of 47.9% MFI ratio) and that for PD-1 binding (loss of 75.3% positive cells and of 53.9% MFI ratio) were significantly observed on day 4 at that seeding cell density (13 × 10^3/cm^2) (Fig. 6B–C). CD10 expression level remained stable from day 1 to day 14 of culture (loss of 3.7% CD10$^+$ cells and of 2.3% MFI ratio) (Fig. 6B–C). We controlled whether the loss of expression level of PD-1 ligands was related to changes in RNA copy number along the culture-time. CD10 was kept as a reference molecule. The copy number of PD-1 ligands and CD10 was assessed *via* droplet digital PCR (ddPCR) that is more sensitive than real-time PCR and enables the absolute quantitation of nucleic acids. The copy numbers/μL increased from day 1 to day 14 for PD-L1, PD-L2, and CD10 in the three γ-FF donors (Fig. 6A). ddPCR shows an increase of the PD-1 ligand gene expression levels suggesting that the observed progressive loss of PD1 ligand cell surface expression cannot be due to an altered transcription.

In order to exclude a loss of cell viability/integrity during the 14 d of culture, we performed detailed analyses of DAPI exclusion, Annexin V binding and senescence. Through all the study, PD-1 ligand expression was studied on DAPI$^-$ adherent γ-FFs, thus the loss of PD-L1 and PD-L2 cannot be related to a loss of viability (Fig. S6A-B). Furthermore, Annexin V binding to phosphatidylserine (PS) translocated to the outer cellular surface was analyzed on DAPI$^-$ cells and revealed that the cells were 61.8±7.1% Annexin V$^+$ on day 1, 32.4±3.0% on day 4 and 19.8±4.6% on day 14 (Fig S6C–D). As expected, because FFs were γ-irradiated adherent cells were all senescent as revealed by senescence-associated β-galactosidase (SA-β-gal)

activity (Fig S6E–G) and γ-FFs remain metabolically active and resistant to apoptosis as described.[40]

We next examined whether this loss of PD-1 ligand expression was dependent on cell seeding density. γ-FFs were cultured at different densities (from 7 × 10^3/cm^2 to 140 × 10^3/cm^2) and PD-1 ligand expression was analyzed on day 1 (reference day with optimal expression) and day 4 of culture (Fig. 7). After 4 d of culture, γ-FFs showed a significant decrease of both PD-1 ligand expression at the seeding concentration of 35 × 10^3/cm^2 (Fig. 7A3–4, B3–4) (loss of 49.6% of PD-L1$^+$ cells and 48.7% of PD-L2$^+$ cells). On day 4, the loss of PD-1 ligand expression was observed from the lowest (35 × 10^3/cm^2) to the highest (140 × 10^3/cm^2) seeding concentrations, with a nearly complete loss of expression at the highest seeding density (Fig. 7A1–2, B1–2). These data indicated that the loss of PD-1 ligand expression on γ-FFs was culture time-dependent and cell-seeding density-dependent.

Loss of PD-L1 and PD-L2 expression on γ-irradiated infant foreskin fibroblasts involved matrix metalloproteinases 9 and 13

In order to decipher the mechanisms of PD-1 ligand loss, we then investigated whether PD-L1 and PD-L2 would undergo extracellular domain proteolytic cleavage by enzymes endowed with MMP-like proteolytic activity that would be secreted by cultured γ-FFs. At first, in order to mimic MMP-proteolytic activity, we selected three enzymes: (i) a highly purified collagenase (CLSPA) with collagenase activity similar to that of the MMP-1, MMP-8 and, MMP-13 sub-group, (ii) Dispase II$^®$ with a proteolytic activity found in the gelatinase MMP-2 and MMP-9 sub-group, and (iii) Thermolysin with additional enzymatic activities such as aspartyl proteinase-like activity found in the Collagenase-3/MMP-13.

The highly purified collagenase (CLSPA) had no effect on PD-1 ligand expression nor on PD1-Fc binding on γ-FFs (Fig. 8A–B). In contrast, pre-incubation with Dispase II$^®$ resulted in a complete loss of PD-L2 detection and a strong decrease of PD-1-Fc binding (17±2.1% of PD-1-Fc$^+$ cells with 2 U/mL Dispase II$^®$), while PD-L1 expression remained nearly unchanged (68.2±3.1% of PD-L1$^+$ cells with 2 U/mL Dispase II, *versus* 80±1.6% of PD-L1$^+$ cells without enzymatic treatment) (Fig. 8A–B). Using 200 μg/mL Thermolysin, both PD-1 ligands were strongly cleaved (37.6±3.0% of PD-L1$^+$ cells; 0.2±0.06% of PD-L2$^+$ cells) resulting in complete loss of PD-1 binding (0.7±0.4% of PD-1-Fc$^+$ cells) (Fig. 8A–B). PD-L2 and consequently, PD-1-Fc fusion protein binding, were more sensitive to cleavage in presence of Thermolysin than PD-L1 (0.9± 0.1% of PD-L2$^+$ cells and 28.9±3.5% of PD-1-Fc$^+$ cells *vs.* 78.9±3.8% of PD-L1$^+$ cells in presence of 50 μg/mL Thermolysin) (Fig. 8B). Similar pattern of cleavage by the three enzymes (collagenase/CLSPA, Dispase II$^®$, and Thermolysin) was obtained when γ-FFs were pre-fixed with 2% PFA confirming that PD-L1 and PD-L2 expression but not CD10 expression are regulated through proteolytic cleavage (Fig. S7). This demonstrated that the expression of PD-1 ligands is affected by enzymes with aspartyl proteinases and to a lesser extent, gelatinase-like MMP activities (in particular PD-L2 molecule was cleaved by Dispase II$^®$), but not collagenase activities.
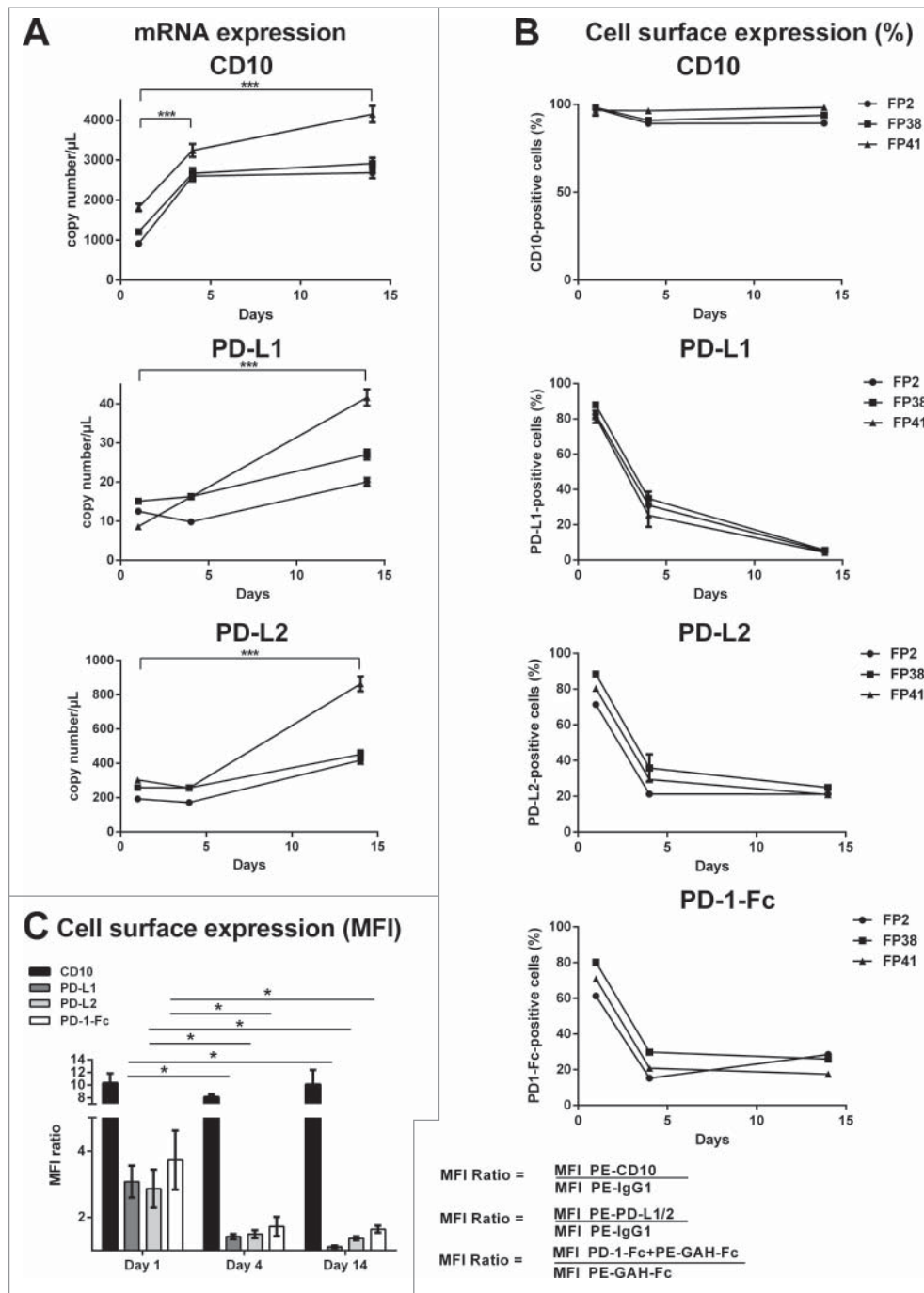
Figure 6. PD-L1, PD-L2, and CD10 transcript quantitation by droplet digital PCR and loss of PD-L1 and PD-L2 expression, and of the capacity to bind PD-1-Fc fusion protein on 30 Gray-irradiated infant foreskin fibroblasts after 4 d and 14 d of culture. Under similar seeding cell density ($13 \times 10^3/cm^2$) γ-FFs (three donors) were maintained in culture for 1, 4, and 14 d (A) Purified total RNA of γ-FFs were examined. All RNAs were quantified by droplet digital PCR and all transcript concentrations are given in copy number/μL (B) Frequency of CD10^{+}, PD-L1^{+}, and PD-L2^{+} cells and frequency of positive cells showing a binding to PD-1-Fc at different times of culture were detected by flow cytometry. (C) Mean fluorescence intensity (MFI) ratio = MFI of cells after labeling with anti-CD10 PE-mAb, anti-PD-L1 PE-mAb, and with anti-PD-L2 PE-mAb: MFI of cells incubated with PE-IgG$_1$ isotype. MFI ratio = MFI of cells after binding with PD-1-Fc fusion protein + PE-conjugated goat anti-human immunoglobulin Fc portion (PE-GAH-Fc):MFI of cells incubated with PE-GAH-Fc. Summation data of three γ-FF donors are shown and representative of n = 3 independent experiments. Bars represent the SD. $^*p < 0.05$, $^{***}p < 0.001$.

We controlled the cellular and molecular specificity of collagenase/CLSPA, Dispase II®, Thermolysin activities on 2% PFA-pre-fixed monocyte-derived dendritic cells (Mo-DCs). Similarly to γ-FFs, PD-L1 expression and PD-1-Fc binding are negatively regulated by a high concentration of Thermolysin (>100 μg/mL). CD80 and CD86 expression underwent no significant downregulation with the three enzymes.(Fig. S8).

To further define which MMP-subgroup contributes to PD-1 ligand expression, we used MMP inhibitors with different specificities. As shown in Fig. 9 (Fig. 9A1–2), only the MMP-13 specific inhibitor (CL82198) significantly ($p < 0.05$) restored PD-L1 expression ($20.6\pm5.9\%$ recovery of the frequency of PD-L1^{+} cells from day 1 to day 4 in presence of 12 μg/mL CL82198) when compared to the other
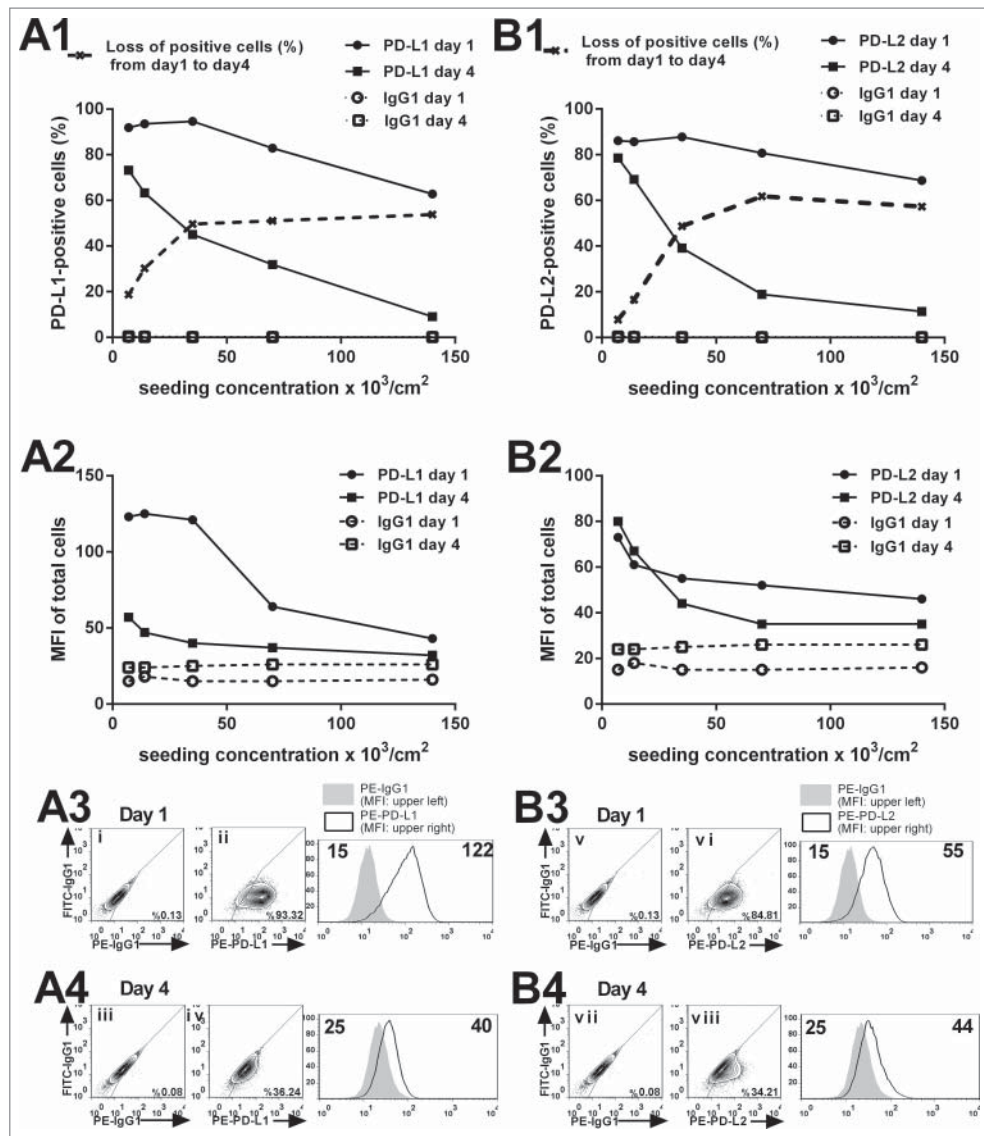
Figure 7. High seeding density of 30 Gray-irradiated infant foreskin fibroblasts favored the loss of PD-L1 and PD-L2 expression between day 1 and day 4 of culture. Under different seeding cell concentrations (7×10^3; 14×10^3; 35×10^3; 70×10^3; $140 \times 10^3/cm^2$), γ-FFs were maintained in culture for 1 and 4 d. Expression levels of PD-1 ligands were detected by flow cytometry. (A1, B1) Frequency of PD-L1 (A1) and PD-L2 (B1) positive cells, and isotype controls (PE-IgG$_1$). Loss of positive cells was calculated between day 1 and day 4 at each seeding density (dotted line). (A2, B2) Mean fluorescence intensity (MFI) of positive cells after labeling with anti-PD-L1 PE-mAb (A2) and with anti-PD-L2 PE-mAb (B2). (A3, A4, B3, B4) For a seeding concentration of $35 \times 10^3/cm^2$, representative dot-plots showed isotype control (i,iii) and PE-PD-L1 mAb (ii,iv) on γ-FFs on day 1 (A3) and day 4 (A4), respectively. Representative flow histogram overlay showed isotype control (filled histograms) with MFI value in upper left and PE-PD-L1 mAb (open histograms) with MFI value in upper right. Representative dot-plots showed isotype control (v,vii) and PE-PD-L2 mAb (vi,viii) on γ-FFs on day 1 (B3) and day 4 (B4), respectively. Representative flow histogram overlay showed isotype control (filled histograms) with MFI value in upper left and PE-PD-L2 mAb (open histograms) with MFI value in upper right. Cytometry data are representative of n = 2 independent experiments.

MMP inhibitors tested (actinonin, SB3CT, NNGH, Z-Pro-Leu-Gly-NHOH and GM6001) (Fig. 9A1). In contrast, PD-L2 expression was partially restored by three MMP inhibitors ($22.9 \pm 1.7\%$ recovery for CL82198, $12.2 \pm 3.0\%$ for actinonin, and $12.7 \pm 0.2\%$ for NNGH) (Fig. 9B1). For both PDL1 and PDL2, similar patterns were observed on day 4 only and CL82198 significantly ($p < 0.05$) restored their expression when compared to the other MMP inhibitors. (Fig. 9A2, B2)

As the expression of both PD-1 ligands was significantly restored by the specific inhibitor of MMP-13 (CL82198), we suggested that MMP-13 was implicated in the shedding/cleavage of PD-L1 and PD-L2 on the γ-FFs.

PD-L1 and PD-L2 cleavage by exogenous MMP-9 and MMP-13 on γ-irradiated infant foreskin fibroblasts reverts apoptotic signals on mitogen-activated T cells

Based on above results, we focused our interest on the MMP-9 with a gelatinase activity, and the MMP-13 with wider proteolytic capacities.[41-43] To block endogenous MMPs, γ-FFs were pre-fixed with 2% PFA. Both MMP-9 and MMP-13 were found to partially but significantly cleave PD-L1 and PD-L2. The percentage of PD-L1$^+$ fixed γ-FFs decreased from $48.6 \pm 2.8\%$ to $39.4 \pm 0.1\%$ and to $31.1 \pm 2.01\%$ in presence of MMP-9 and MMP-13, respectively. The percentage of PD-L2$^+$ cells decreased from $49.8 \pm 0.2\%$ to $40.2 \pm 2.7\%$ and to $36.8 \pm 0.4\%$ in presence of MMP-9 and MMP-13, respectively
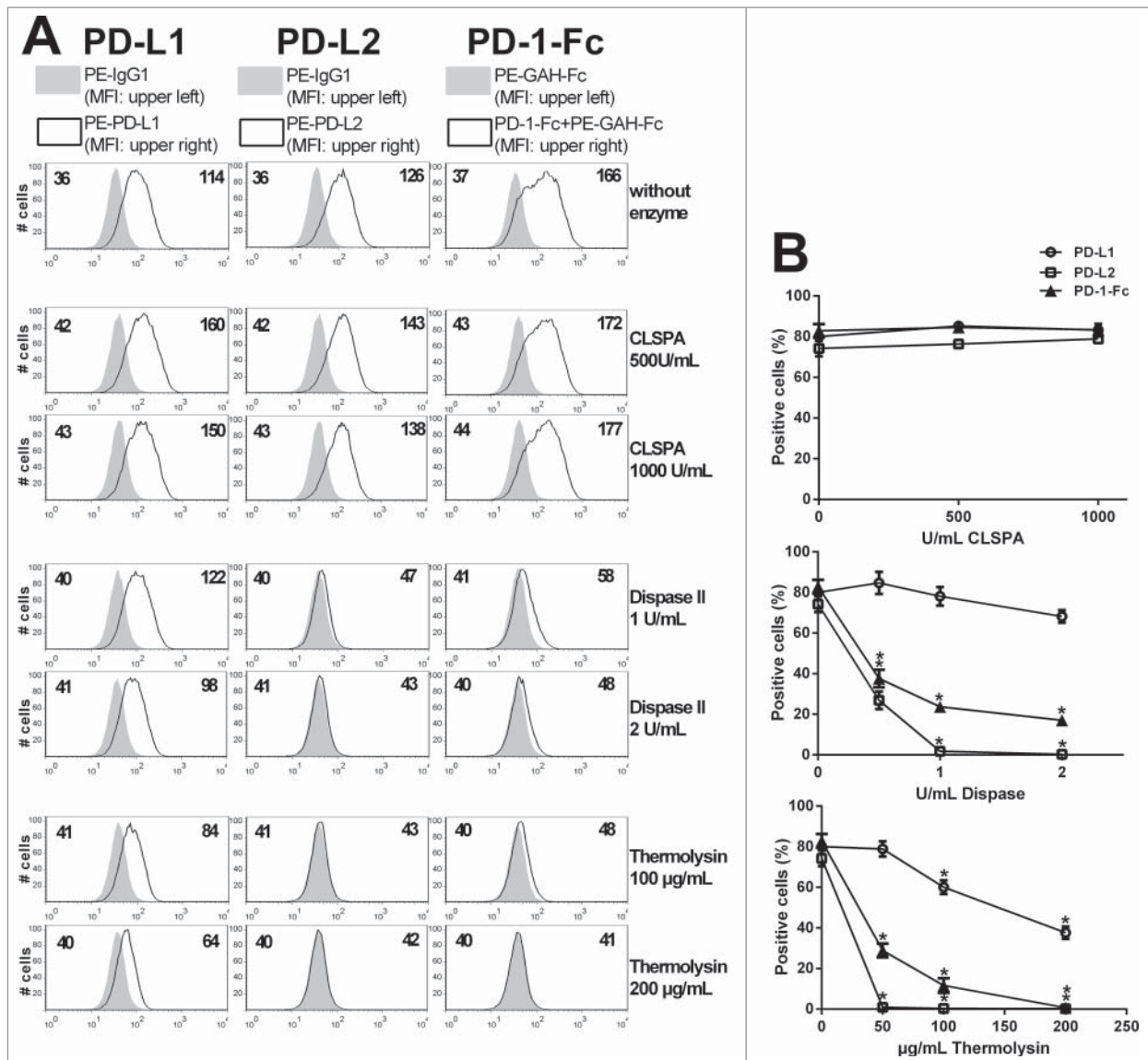
Figure 8. Cleavage/shedding of PD-L1, PD-L2, and PD-1-Fc binding by exogenous enzymes with MMP-like activities. After 1 day of culture, γ-FFs were maintained at 37°C in suspension in presence of different concentrations of chromatographically purified collagenase (CLSPA, 500 and 1000 U/mL), Dispase II® (0.5, 1, and 2 U/mL), and Thermolysin (50, 100, and 200 μg/mL) for 1 h. Expression levels of PD-1 ligands and binding capacity of PD-1-Fc were detected by flow cytometry. (A) Representative flow histogram overlay showed isotype control (filled histograms) with MFI value in upper left and PE-PD-L1 mAb/PE-PD-L2 mAb (open histograms) with MFI value in upper right. Representative flow histogram overlay showed PE-GAH-Fc control (filled histograms) with MFI value in upper left and PD-1-Fc + PE-GAH-Fc (open histograms) with MFI value in upper right. (B) Frequency of PD-L1^{+}, PD-L2^{+} cells, and PD-1-Fc-binding cells after cleavage by collagenase (CLSPA), Dispase II®, and Thermolysin. Data are representative of n = 3 independent experiments. Bars represent the SD. $^{*}p < 0.05$.

(Fig. 10A–B). Similarly, both MMPs significantly decreased the percentage of PD-1-Fc^{+} fixed γ-FFs from 36.0 ± 2.2% to 21.7 ± 2.6% and to 21.0 ± 0.9% in presence of MMP-9 and MMP-13, respectively (Fig. 10C). This result showed that PD-1-binding domains of both PD-1 ligands are partially but significantly cleaved by MMP-9 and by MMP-13.

We controlled the cellular and molecular specificity of MMP-9 and MMP-13 activities on 2% PFA-pre-fixed Mo-DCs. Both MMP-9 and MMP-13 were found to partially but significantly decrease the percentage of PD-1-Fc^{+} PFA-prefixed Mo-DC from 49.9 ± 2.2% to 39.5 ± 3.6%, and to 23.7 ± 0.1% in presence of MMP-9 and MMP-13, respectively (Fig. S9). CD80, CD86, and PD-L1 expression was non-significantly decreased through both MMP proteolytic cleavage.(Fig. S9).

We then assessed the impact of MMP-9 and MMP-13 on γ-FFs-mediated early apoptosis of PHA-activated T cells. MMP-9 treatment of γ-FFs induced a decrease in the percentage of early apoptotic T cells, for both γ-FF:T cell ratios tested. The percentage of early apoptotic CD4^{+} T cells decreased from 26.9 ± 3.3% to 18.2 ± 0.3%, $p < 0.05$ with the ratio 5 γ-FF:100 T cells while that of CD8^{+} T cells decreased from 50.5 ± 9.6% to 28.5 ± 0.6%, $p < 0.05$ with a similar ratio (Fig. 10D–E). Similarly, γ-FFs-treatment by MMP-13 induced a decrease in the percentage of early apoptotic CD4^{+} T cells (from 26.9± 3.3% to 17.4 ± 0.1%, $p < 0.05$ with the ratio 5 γ-FF:100 T cells and CD8^{+} T cells subset (from 50.5 ± 9.6% to 26.8 ± 1.4%, $p < 0.05$ with a similar ratio) (Fig. 10D–E). These data demonstrate that MMP-9 and MMP-13 cleaved PD-1 ligands
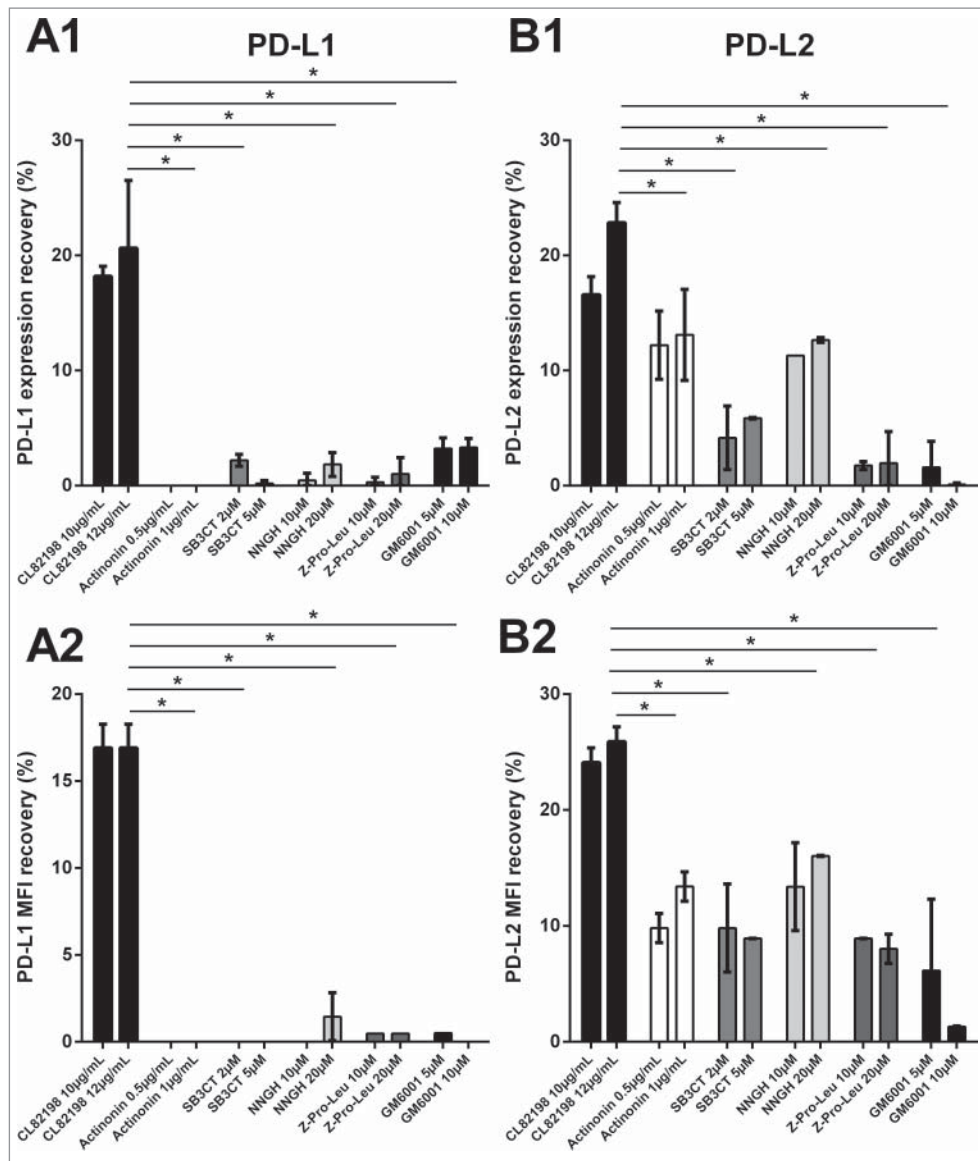
Figure 9. The specific MMP-13 inhibitor CL82198 significantly restored PD-L1 and PD-L2 expression on 30 Gray-irradiated infant foreskin fibroblasts maintained in culture for 4 d. After 1 day of culture at 37°C, γ-FFs were further cultured for 4 d at 37°C in presence or not of MMP inhibitors (without any medium change). Six MMP inhibitors were tested at two different concentrations. Expression levels of PD-L1 and PD-L2 were detected by flow cytometry on γ-FFs on day 1 and day 4. (A1, B1) Recovery (%) of the frequency of PD-L1$^+$ and PD-L2$^+$ cells after 4 d of culture in presence of the MMP inhibitors. (A2, B2) Recovery (%) of mean fluorescence intensity (MFI) value of the PD-L1$^+$ and PD-L2$^+$ cells cultured in presence of MMP inhibitors for 4 d. Results are representative of n = 4 independent experiments. Bars represent the SD $^*p < 0.05$ between CL82198 12 μg/mL (black histogram) and all other concentrations of MMP inhibitors tested (Actinonin, SB3CT, NNGH, Z-Pro-Leu-Gly-NHOH, GM6001).

(Fig. 10A–C) and consequently, abrogate γ-FFs-induced T cell apoptosis.(Fig. 10D–E)

Carcinoma-associated fibroblasts behave like PD-1 ligand-depleted fibroblasts

We compared the behavior of isolated and irradiated-carcinoma-associated fibroblasts (γ-CAFs) to emphasize the biological relevance of MMPs in a cancer microenvironment. CAFs were isolated from the connective tissue of fresh tumors from patients diagnosed with primary breast carcinoma. CAFs followed similar irradiation protocol as FFs. We showed that γ-CAFs expressed significantly lower levels of PD-L1 and PD-L2, and a low binding of soluble PD-1-Fc fusion protein compared to γ-FFs (Fig. 11A). Among 13 different γ-FFs and 8

γ-CAFs studied in the same period, the frequency of PD-1-Fc$^+$ cells was 61.6 ± 10.9% for γ-FFs *versus* 13.0.7 ± 15.2% for γ-CAFs, the percentages of PD-L1$^+$ cells were 61.1 ± 13.4% for γ-FFs *vs.* 14.7±17.6% for γ-CAFs, and the percentages of PD-L2$^+$ cells were 66.9 ± 11.6% for γ-FFs *versus* 9.43 ± 11.8% for γ-CAFs.(Fig. 11A)

The effect of γ-FFs and γ-CAFs on CD3$^+$ T cell proliferation in presence of the mitogen PHA was examined. We observed that γ-FFs but not γ-CAFs (two donors) significantly ($p < 0.05$ at both ratios) inhibited PHA-stimulated CD4$^+$ and CD8$^+$ T-cell proliferation by reducing the absolute numbers of CD4$^+$ T cells and CD8$^+$ T cells (Fig. 11B). As previously shown in Fig. 5A1–2, a pre-incubation of γ-FFs with both blocking anti-PD-1 ligand mAbs, partially restored PHA-stimulated CD4$^+$ T cell and CD8$^+$ T cell proliferation ($p < 0.05$ at both
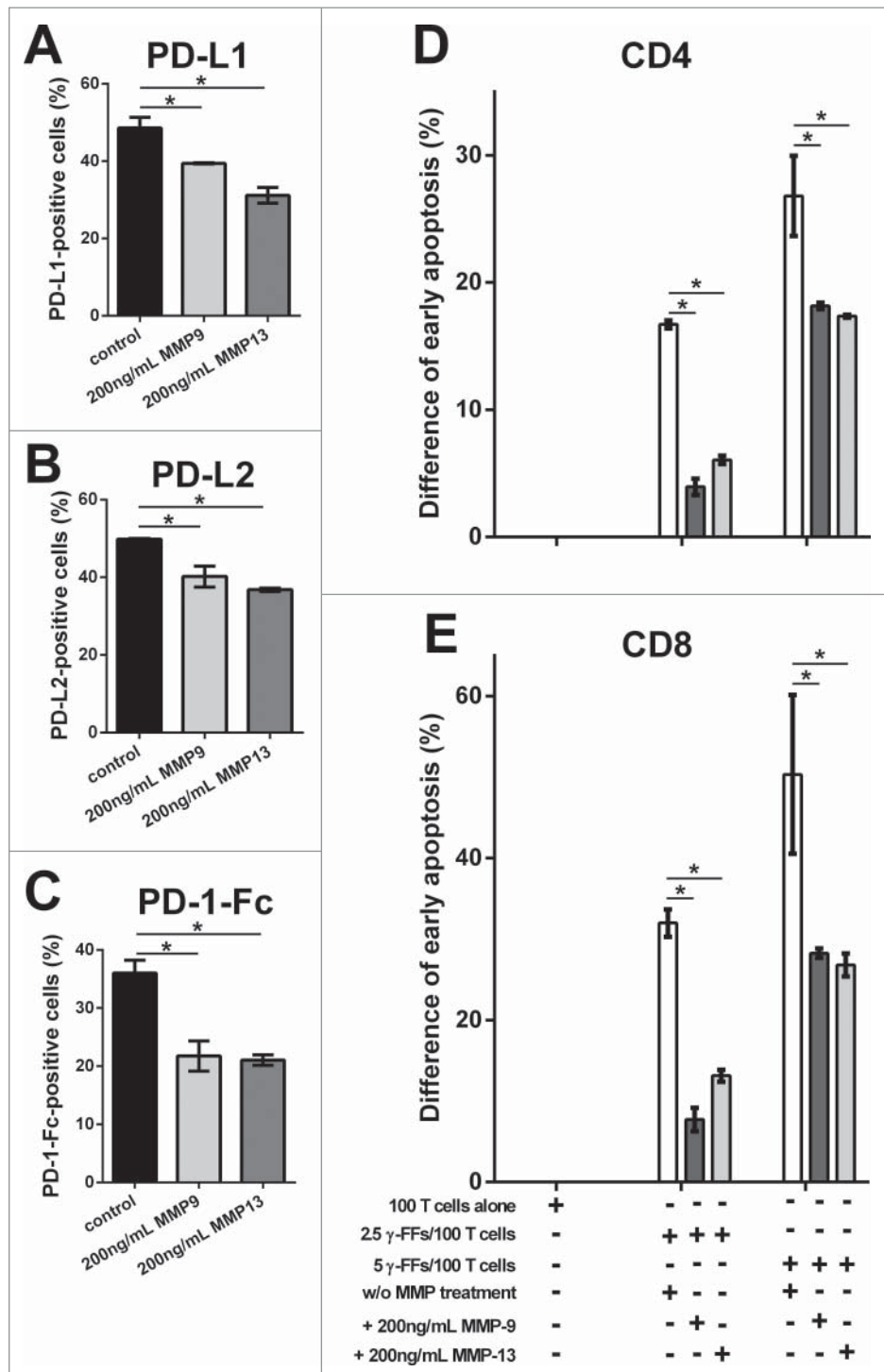
Figure 10. PD-L1 and PD-L2 cleavage by exogenous MMP-9 and MMP-13 on 30 Gray-irradiated infant foreskin fibroblasts reverts apoptotic signals on mitogen-activated T cells. (A–C) After 2 d of culture in presence of 100 ng/mL TNFα, plated γ-FFs were fixed with 2% PFA then after washing were incubated at 37°C in presence of APMA-activated pro-MMP-9 and pro-MMP-13 in culture medium (1% FCS) for 24 h. Expression levels of PD-1 ligands and binding capacity of PD-1-Fc (3 μg/mL) were detected by flow cytometry. Frequency of PD-L1+, PD-L2+ cells (A, B), and PD-1-Fc-binding cells (C) was calculated after 24 h incubation in presence or not of exogenous MMP-9 and MMP-13. Results are representative of two independent experiments. Bars represent the SD. *$p < 0$ .05. (D–E): After 2 d of culture, γ-FFs were directly incubated at 37°C in presence or not of APMA-activated pro-MMP-9 and pro-MMP-13 in culture medium (1% FCS) for 24 h. CD3+ T cells were added and early T cell apoptosis after 17 h-PHA activation was determined by the difference of percentage of early apoptotic CD3+ T cells (DAPI⁻ T cells/Annexin V+) in presence or in absence of γ-FFs at two ratios of 2.5 γ-FFs:100 T cells and 5 γ-FFs:100 T cells. After PHA activation in the conditions as indicated, T cells were co-labeled with anti-CD4-FITC mAb and anti-CD8-PerCP-Cy5.5 mAb, stained with PE-Annexin V and, then analyzed by flow cytometry. Results are representative of n = 2 independent experiments. Bars represent the SD *$p < 0$ .05.

ratios) (Fig. 11B). These results show that γ-CAFs, did not suppress but even slightly enhance T cell proliferation. Thus, γ-CAFs behave like γ-FFs that were pre-incubated with both blocking anti- PD-1 ligand mAbs.

We controlled whether the loss of PD-1 ligand expression and the impaired immunosuppression on T cell by γ-CAFs compared to γ-FFs were due to a higher secretion of MMPs and consequently, cleavage of PD-1 ligands on γ-CAFs. γ-FFs
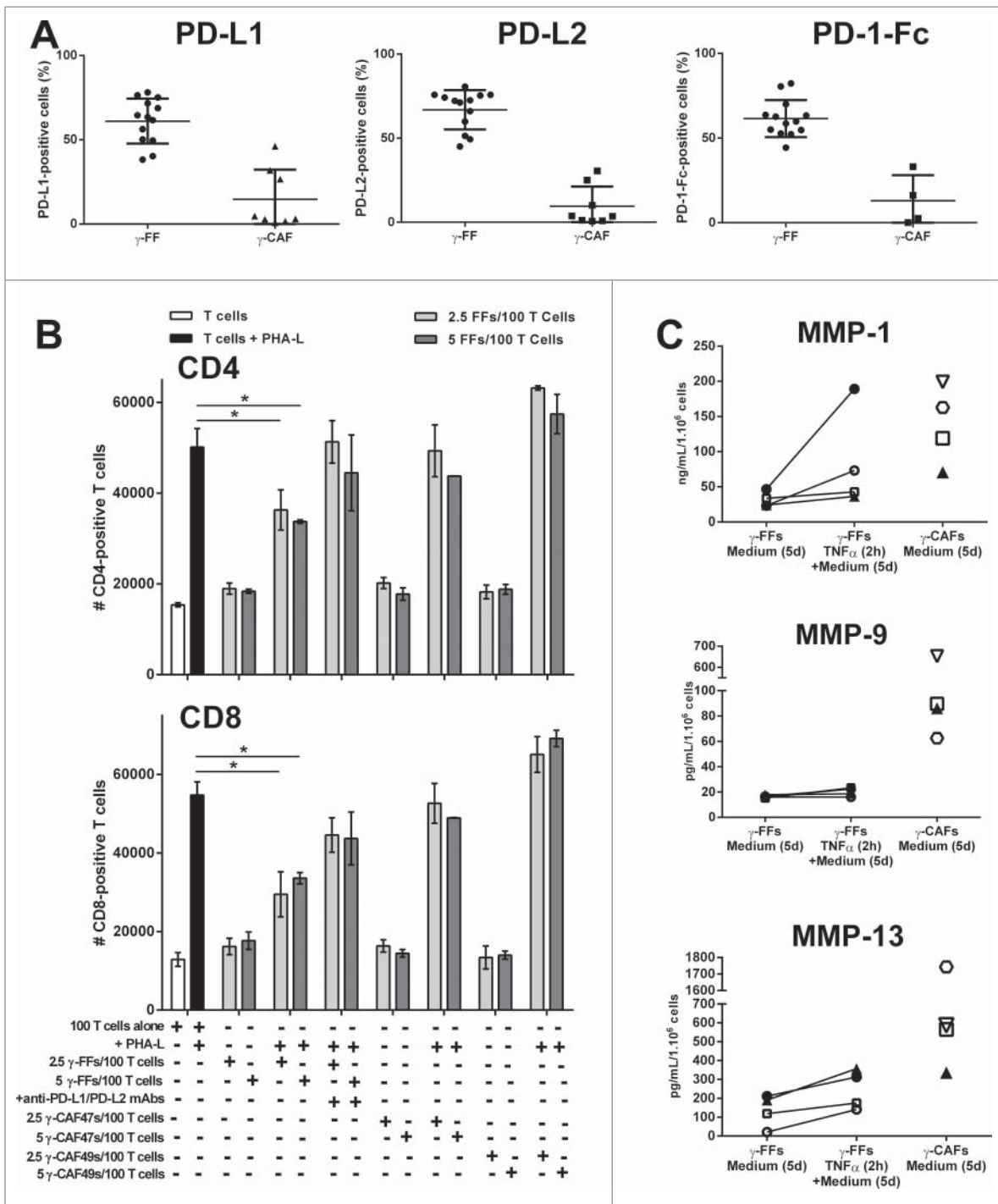
Figure 11. Comparison between 30 Gray-irradiated Carcinoma Associated Fibroblasts (γ-CAFs) and 30 Gray-irradiated infant foreskin fibroblasts (γ-FFs) in their PD-1 ligand expression, inhibitory capacity of mitogen-induced T cell proliferation, and MMP-1, MMP-9, and MMP-13 secretion capacity. (A) Frequency of PD-L1 and PD-L2 expression and of PD-1-Fc fusion protein binding on γ-FFs (n = 13 donors) and γ-CAFs (n = 8 donors). The frequency of cells expressing PD-L1, PD-L2, and PD-1-Fc binding was analyzed by flow cytometry after 24 h of culture under identical seeding concentrations. Each symbol represents a different donor. Bars represent mean values $\pm$ SD. (B) γ-CAFs do not reduce the numbers of CD3$^+$ T cells after 7 d of co-culture in presence of the polyclonal mitogen PHA-L (0.5 μg/mL). PD-L1 and PD-L2 blockade by anti-PD-1 ligand mAbs (clone 29E23A3 + clone 24F10C12) only reverts the inhibition of T cell proliferation by γ-FFs. Data represent the numbers of CD4$^+$ cells and CD8$^+$ T cells within the CD3$^+$ T cells. Bars represent SD $^*p$ < 0 .05. (C) Quantitative determination of MMP-1, MMP-9, and MMP-13 released by γ-FFs (n = 4 donors) and γ-CAFs (n = 4 donors). γ-FFs and γ-CAFs were plated for 4 h in D-MEM supplemented with 10% FCS and D-MEM/F-12:1/1 supplemented with 10% FCS, respectively at 37°C. Only γ-FFs were incubated for 2 h at 37°C in presence of 100 ng/mL TNFα in D-MEM supplemented with 1% FCS while γ-CAFs were directly incubated in D-MEM/F-12:1/1 supplemented with 1% FCS. Both γ-FFs and γ-CAFs were maintained for 5 d in their respective medium supplemented with 1% FCS (without any medium change). Supernatants (duplicate) were analyzed with Magnetic Luminex® Performance Assay test (Human MMP-1, MMP-9, and MMP-13).

and γ-CAFs were maintained in similar culture conditions and MMP-1, MMP-9, and MMP-13 were measured in supernatants by Magnetic Luminex® assay (Fig. 11C). A pre-treatment of

γ-FFs with TNFα for 2 h at 37°C enhanced the secretion of MMP-1 (31.9 $\pm$ 10.9 ng/mL/1 $\times$ 10^6 cells *vs.* 85.4 $\pm$ 61.5 ng/mL/1 $\times$ 10^6 cells in presence TNFα) and MMP-13 (135.1 $\pm$

85.7 pg/mL/1 × 10^{6} cells *versus* 246.2 ± 104.9 pg/mL/1 × 10^{6} cells in presence of TNFα). Without TNFα treatment, γ-CAFs showed a 2–4-fold higher level in MMP-1 secretion, 10-fold in MMP-9 and 3–6-fold in MMP-13 compared to γ-FFs (Fig. 11C). These results suggest that any environmental conditions favoring MMP release by fibroblasts may impair their immunosuppressive capacities by alteration of the PD-1/PD-1 ligand pathway.

Discussion

Similarly to MSCs[1] fibroblasts are not just passive structural cells but may play an active role in immune cell functions through early apoptosis induction of activated T cells in a PD-1/PD-1 ligand-dependent manner. We provide evidence, for the first time to our knowledge, that an MMP activity can prevent early apoptosis of activated CD3^{+} T cells through PD-1 ligand cleavage on fibroblast cell membrane. We showed that both γ-irradiated and non-irradiated FFs express the co-inhibitory molecules PD-L1 and PD-L2. While the expression of PD-L2 in normal conditions has been thought to be predominantly restricted to professional APCs such as DCs and macrophages,[25,27] the expression of PD-L1 appears more ubiquitous. PD-1 ligand expression and functions linked to attenuating T cell response, promoting T cell tolerance or preventing autoimmunity were well documented on hematopoietic cells.[12,44] In contrast, conflicting data were reported on the expression and functions of PD-1 ligands by murine/human bone marrow-MSCs and fibroblasts. After isolation and *in vitro* expansion, mesenchymal/stromal cells from different cellular sources may express from negligible to high levels of PD-L1 and PD-L2 molecules.[45] Furthermore, PD-L1 expression by human normal dermal fibroblasts/myofibroblasts has been reported.[31] Indeed, PD-L1 and PD-L2 were shown to be constitutively expressed by fibroblasts/myofibroblasts in the normal colonic mucosa both *in situ* and in culture[32] and by carcinoma-associated fibroblasts in non-small cell lung tumor.[11] Furthermore, we clearly demonstrate that PD-L1 expression on γ-FF was selectively upregulated by IFNγ as reported on murine MSCs,[46] human bone marrow-derived MSCs,[12] human carcinoma-associated fibroblasts in non-small-cell lung tumor,[11] and placenta-derived MSCs,[47] while PD-L2 expression and PD1-Fc binding was mainly increased in presence of IFNγ, TNFα or IL-1α, as well as in combinations. These observations are in agreement with previous studies showing that PD-L1 expression can be upregulated by both type I and type II interferons[23,48] but also induced by intrinsic signals such as activation of EGFR[49] and KRas[50] signaling pathways, while PD-L2 expression was reported to be potently upregulated on non-hematopoietic cells by IFNγ and TNFα.[51,52] It is currently accepted that PD-1 ligands are upregulated by a variety of hematopoietic and non-hematopoietic cells in the presence of strong inflammatory signals presumably to prevent collateral damage induced by potentially destructive Th1/Th17 T cell responses.[12,32,51–53]

The expression of PD-L1 and PD-L2 of γ-FFs on the outcome of their interactions with PD-1^{+} effector T cells was demonstrated by the binding of PD-1-Fc that was potently blocked by anti-PD-L2 mAb alone compared to anti-PD-L1 mAb alone although both mAbs were required to completely abrogate the binding of PD-1-Fc protein. Our observation is also in agreement with a previous study[37] demonstrating by surface plasmon resonance and cell surface binding[37] that, although both PD-1 ligands cross-compete to bind to their receptor PD-1, PD-L1 binding to PD-1 involves complex conformational changes while PD-L2 interacts in a direct manner with PD-1, revealing distinct molecular mechanisms of interaction between PD-1 and its ligands.[28] Furthermore, the relative affinity of PD-L2 for PD-1 is 2–6-fold higher than that of PD-L1.[29] PD-L2 expressed at the same level of PD-L1 would be expected to outcompete PD-L1 for the binding of PD-1. Nevertheless, PD-L1 remains the primary binding ligand of PD-1 by the fact that PD-L2 is generally expressed at lower basal levels.[12,54,55] While PD-L1 is considered as the dominant negative inhibitory molecule, in our study PD-L2 on infant γ-FFs appeared as a critical suppressive molecule in the binding to PD-1 receptor. Indeed, the blockade of both ligands is required for optimal restoration of the mitogen-activated CD8^{+} T cell proliferation instead of the single blockade of either PD-L1 or PD-L2 (data not shown).

We demonstrated that γ-FFs inhibited PHA-stimulated T cell proliferation through induction of apoptosis, and that blocking both PD-L1 and PD-L2 significantly reduced early apoptosis of PHA-activated T cells and consequently abrogate inhibition of T cell activation and proliferation. This finding complements previous observation (i) from Curiel et al.[56] showing that, in human ovarian carcinoma, blockade of PD-L1 on differentiated myeloid DCs (MDCs) improves T cell activation by upregulation of MDC IL-12 and downregulation of IL-10 and (ii) from Nazareth et al.[11] showing that, in human non-small-cell lung cancer, blockade of PD-L1 and/or PD-L2 on tumor-associated fibroblasts reverse the suppressed tumor-associated T cell activation. Many reports have shown that PD-1 engagement inhibits T cell activation and suppresses immune response by inducing apoptosis, anergy, unresponsiveness, and functional exhaustion of T cells.[12] Previous reports emphasize the role of PD-1 on either cell cycle arrest[27] or T cell death[53] PD-1 might directly engage a death pathway or indirectly by downregulating survival signals and growth factors or synergizing with death pathways. PD-1 ligation inhibits expression of the cell survival gene *bcl-xL* and several growth factors.[13] The outcome of PD-1/PD-L1 interactions on T cell expansion and survival might also depend on the type of APCs that interact with the T cells. Indeed, in absence of CD28 ligation (γ-FFs are CD80/86[−]), the engagement of PD-1 may preferentially favor activation-induced cell death as previously suggested for the PD-L1^{+} HepG2.2.15 cell line, promoting CD8^{+} T cell apoptosis.[57]

Because activated and *in vitro* cultured fibroblasts/MSCs are reported to produce important levels of TGFβ1–3,[58] IL-10,[59,60] Prostaglandin E2,[61] and IDO,[6,62] we do not exclude that the interaction between γ-FFs and PHA-activated T cells may trigger release of these suppressive molecules by fibroblasts and these, in turn, may contribute to inhibit T cell proliferation.

Although most studies agree that soluble factors are involved in inhibition by MSCs, controversial results render these molecular mechanisms rather elusive in experiments involving fibroblasts.[6] Furthermore, in contrast to MSCs, γ-FFs did not express Fas Ligand (data not shown) and would not be

capable to induce early apoptosis of activated T cells through Fas/Fas ligand interactions.[45] In contrast to normal PD-L1[+]/PD-L2[+] human colonic myofibroblasts and fibroblasts, our results did not support the notion that PD-L1/-L2-mediated suppressive functions are due to inhibition of IL-2 production.[32]

Furthermore, our work proved that PD-L1 and PD-L2 are spontaneously expressed by FFs and are lost as a function of culture-time and cell-seeding density. ddPCR data showed no evidence of alterations at the transcriptional level of the molecules. For the first time, to our knowledge, we demonstrated proteolytic cleavage of PD-L1 and PD-L2 occurring through the release of MMPs by the γ-FFs. Consequently, the loss of extracellular PD-1-binding domain leads to the loss of γ-FFs-mediated T cell apoptosis. Using (i) different purified enzymatic activities e.g. collagenase, Dispase II®, and Thermolysin, (ii) a specific MMP-13 inhibitor and MMP inhibitors with broader specificities, and (iii) recombinant exogenous MMP-9 and MMP-13, we demonstrated that while PD-L1 was selectively cleaved by MMP-13, PD-L2 was sensitive to a broad range of MMP activities. MMP-13 shares additional enzymatic activity with both MMP-subgroups of collagenases and gelatinases and was also described as a protease able to cleave certain chemokines (MCP-3/CCL7, SDF-1/CXCL12), collagen IV, and to activate pro-MMP-2, pro-MMP-9, and pro-MMP-13.[63] As previously reported, MMP-13 can be produced by skin fibroblasts and breast-cancer-cell-associated myofibroblasts.[64] Our hypothesis of γ-FFs as a source of MMP-13 was substantiated by in vitro experiments showing MMP-13 release in γ-FFs treated or not with TNFα although γ-FFs were less efficient than γ-CAFs in MMP-9 and MMP-13 secretion. Finally, we clearly showed evidence that cleavage activity by exogenous MMP-13 not only led to a partial loss of PD-L1 and PD-L2 expression but also to a loss of the extracellular PD-1 binding domain that was found linked to the reversal of early apoptosis of PHA-activated T cells. We showed that such MMP-13 cleavage may also concern the PD-1 binding domain present on other hematopoietic cells such as MDC populations. Incidentally, we provide evidence of proteolytic sensitivity of both PD-1 ligands to enzymes used to disrupt basal membranes and dissociate multiple epithelial solid tissues, indicating potential issues with cell surface staining performed following enzymatic tissue disruption.

Studies have described soluble form of PD-L1 (sPD-L1) in culture supernatant and plasma of patients, levels of which correlate with that of cell membrane expression.[65,66] Although binding of sPD-L1 to PD-1 has been reported,[65] based on the fact that only the dimeric form of the recombinant sPD-L1 (PD-L1-Fc fusion protein) activates signaling through PD-1,[66] it is likely that the cleaved form of PD-L1 would function as a PD-1 antagonist. It is worth mentioning that soluble PD-L2 was also described through splice variants, although the biological function of these soluble PD-L2 forms remain unknown.[44,67]

The substrates that can be cleaved by proteinases (MMPs and A Disintegrin And Metalloproteinases (ADAMs)) are proven to be essential for proper immune-cell function.[44,68] MMPs are extracellular zinc-dependent neutral endopeptidases[63] that have many different substrates, and besides ECM

structures, they activate and alter bioactive state of cytokines, chemokines, growth factors, and also affect cell surface receptors, release soluble forms of co-regulatory molecules that may impact immunity. MMPs and ADAMs may serve as activators or inhibitors of immune mediators through several type of proteolytic processing including (i) clipping/cleavage of low-molecular weight chemokine MMPs[69-71] and (ii) shedding which releases an intact ectodomain of the target cell-surface molecule e.g., shedding of the cell-membrane form of TNF[72] and IL-6R by ADAM17; shedding of CD23 or FcεRII by ADAM10.[73]

Shedding of ligands of the B7 family can occur, producing soluble forms that might act as antagonists of the immune response.[74] Similarly, soluble active B7-H3 forms can be released by monocytes, DCs, activated T cells, and B7-H3^{+} carcinoma cells were found able to bind to the B7-H3 receptor on activated T cells, indicating that soluble B7-H3 forms retain biological activity. Although B7-H3 shedding was blocked by a synthetic MMP inhibitor (GM6001), the identity of the specific enzyme(s) is not yet known.[75,76] Similarly to our observation, Schlecker et al.[77] identified ectodomain shedding of B7-H6 by ADAM-10 and ADAM-17 as a novel mechanism of immune escape by tumor cells. Shedding of B7-H6, a ligand for the activating receptor NKp30 abrogates NK-cell activation and consequently NK-cell-mediated killing.[77] Functions of PD-L1/CD80 pathway reside in its complexity of ligand-receptor interactions e.g. PD-L1 binds both PD-1 and CD80, while CD80 interacts with CD28 and CTLA-4 in addition to PD-L1. Selectively, specific attenuation of PD-L1/PD-L2 expression compared to no alteration of the CD80/CD86 tandem through MMP-13 proteolytic cleavage might result in the loss of most of these multiple receptor interactions. Thus, deletion of bidirectional coinhibitory signals to T cells might lead to (i) induction and maintenance of T-cell exhaustion (abrogation of PD-L1/PD-1 interaction) and/or (ii) prevention and reversion of T cell anergy (abrogation of PD-L1/CD80 interaction).[78]

In our study, we suggest that MMP-9/MMP-13 would not have a simplistic role in the degradation of matrix and non-matrix components that would facilitate evasion and migration of cells but would also regulate T cell response by cleavage/shedding of negative regulation molecules implicated in T cell apoptosis. However, although we did not deeply investigate which mechanism, either cleavage or shedding, occurs through MMP-9/MMP-13 proteolysis of membrane-bound PD-L1 and PD-L2 molecules.

The dominant role of PD-1 pathway is to limit the activity of T cells in inflamed peripheral tissues at the time of infection in order to limit tissue damage and risk of autoimmunity.[12,25,79,80] Indeed, PD-1 pathway is believed not to regulate the initial T cell activation stage but rather to control effector T cell activation at the inflammatory site preventing attack of peripheral tissues. While chronic antigen exposure can lead to high levels of persistent PD-1 expression on effector T cells, inflammatory signals in tissues induce PD-1 ligand expression on a variety of cells that down regulate the activity of PD-1^{+} T cells and thus limit collateral tissue damage. Consequently, blockade or elimination of PD-1 ligands leads to exacerbated inflammation associated with severe tissue damage and increase of the magnitude of T cell response and potentially detrimental tissue

destruction. In tumor microenvironment, cancer cells develop resistance mechanisms, including local immune suppression, induction of tolerance, and systemic dysfunction in T cell signaling driving T cells to differentiate into exhausted T cells. Exhausted CD8^{+} T cells express high levels of inhibitory receptors, including PD-1 as the major inhibitory receptor, produce less effector cytokines, and lose the ability to eliminate cancer. Considered as defective memory T cells, the final stage of T-cell exhaustion is the physical deletion by which severely exhausted T cells are cleared in cancer microenvironment mainly through PD-L1-associated T-cell apoptosis. PD-L1 expression inversely correlates with survival of exhausted T cell.[78,81] In complex tumor microenvironment, MMPs (MMP-1, MMP-2, MMP-3, MMP-7, MMP-9, MMP-13, and MMP-14) expressed by both tumor cells and stromal cells are known to cooperate and promote tumor initiation, tumor invasion, metastasis, and angiogenesis.[63] MMP-13 was originally cloned from a human breast tumor cDNA library.[82] Our data depict MMPs as regulators of survival of exhausted T cells. MMP-mediated loss of PD-1-ligand expression on stromal cells would prevent blockade of PD-L1/PD-1 signaling pathway and increase the magnitude of these defective exhausted memory CD8^{+} T cell response.

Furthermore, in light of the potent therapeutic activity of anti-PD-1 and anti-PD-L1 monoclonal antibodies in several incurable cancer pathologies,[17,20-22] these observations represent a novel dimension that would need to be integrated to define prognostic markers of responses to these immunotherapies.

Materials and Methods

Antibodies and reagents

D-MEM (1X) medium with GlutaMAX[TM], 4.5 g/L of D-Glucose, and Pyruvate; D-MEM/F-12 (1:1) (1X) with Gluta-MAX[TM]; RPMI Medium 1640 with GlutaMAX[TM] and 25 mM Hepes; 0.05% Trypsine:EDTA; 10 mg/mL Gentamicin; 10,000 U/mL Penicillin, 10,000 μg/mL Streptomycin; HBSS (1X) solution w/o Ca^{2+}, w/o Mg^{2+}; Hepes (1M) were obtained from Gibco® by Life technologies[TM]. Foetal calf serum (FCS) was obtained from Eurobio Abcys®. Bovine Serum Albumin (BSA) (30% in D-PBS); NaCl; $CaCl_2$, $2H_2O$ and paraformaldehyde were obtained from Sigma-Aldrich®.

Recombinant human (rh) IL-2, rhIL-7, rhIFNγ, rhIL-1alpha, rhIL-4, rhTGF-beta1, and rhIL-17A were from PeproTech[TM]. RhTNF-α was from Miltenyi[TM]. RhPD-1-Fc chimera, pro-form of rhMMP-9, pro-form of rhMMP-13, and GM-CSF were from R&D Systems[TM]. LEAF[TM] (Low Endotoxin, Azide-Free) purified anti-human CD274 (B7-H1, PD-L1), clone 29E.2A3, mouse IgG2b,κ, and LEAF[TM] purified anti-human CD273 (B7-DC, PD-L2), clone 24F.10C12, mouse IgG2a,κ were obtained from BioLegend. Lymphocyte separation medium was obtained from Eurobio AbCys and Percoll[TM]-PLUS was from GE Healthcare-Sweden. MMP inhibitors: CL82198, actinonin, SB3CT, NNGH, Z-Pro-Leu-Gly-NHOH, and GM6001 were from Enzo Life Science. CL82198 is a novel selective inhibitor of MMP-13 (89% inhibition) that binds to the S1′ pocket of MMP-13. CL82198 does not inhibit MMP-1, -2, -3, -7, -8, -9, -10, -12, -14, or ADAM-17/TACE. Actinonin is an inhibitor of MMP-1, -2, -3, -7, -8, -9, -10, -12. Actinonin

would also inhibit MMP-13 but not MMP-14. SB3CT is a competitive inhibitor of MMP-2 and MMP-9 but a weak inhibitor of MMP-1, -3, -7 and ADAM-17/TACE. GM-6001 is a potent broad-spectrum inhibitor of MMPs: MMP-1, -2, -3, -7, -8, -9, -12, -14, -26 and would also inhibits MMP-10, -13, -15, -17, -20, -21, ADAM-17, -19 and others ADAMs. NNGH is a potent inhibitor of MMP3 but would also inhibit MMP-1, -2, -7, -8, -9, -10, -12, -13, -14. Z-Pro-Leu-Gly-NHOH is an inhibitor of collagenases, MMP-2, and MMP-9. Lectin from *Phaseolus vulgaris* (red kidney bean) and leucoagglutinin, PHA-L and *Escherichia Coli* lipopolysaccharide (LPS) were from Sigma-Aldrich®. Chromatographically purified collagenase (code CLSPA) $\geq$ 300 units per mg activity, was obtained from Worthington Biochemical Corporation by Serlabo Technologies. Dispase II®, neutral protease grade II (0.98U/mg) from *Bacillus polymyx* was from Roche Diagnostics and Thermolysin ($\approx$40 U/mg) from *Bacillus thermoproteolyticus rokko* was from Fluka. DMSO and Bafilomycin A1 were used and provided by Sigma Aldrich®. 5-dodecanoylaminofluorescein di-β-D-galactopyranoside (C_{12}FDG) was provided by Life technologies[TM]. For activation of pro-forms of MMP-9 and MMP-13, p-AminoPhenylMercuric Acetate (APMA) was used and provided by Sigma Aldrich®.

Flow cytometry reagents and antibodies

The viable γ-irradiated and non-irradiated FFs and the viable T cells were determined by blue-fluorescent DAPI exclusion staining (Molecular Probes® of Life Technologies).

For phenotype determination of human FFs, the following mouse antibodies were used: phycoerythrin (PE)-conjugated anti-CD10 (Beckman-Coulter, IO-test®, clone ALB1, IgG$_1$), anti-CD34 (BD PharMingen[TM], clone TY/23, IgG$_1$), anti-CD45 (Beckman Coulter, clone J33, IgG$_1$), anti-CD73 (BD PharMingen[TM], clone 581, IgG$_1$), anti-CD80 (Beckman-Coulter, IO-test®, clone MAB104, IgG$_1$), anti-CD86 (Beckman-Coulter, IO-test®, clone HA5.2B7, IgG$_{2b}$), anti-CD90 (BioLegend, clone 5E10, IgG$_1$), anti-CD105 (BD PharMingen[TM], clone 266, IgG$_1$), anti-CD146 (BD PharMingen[TM], clone P1H12, IgG$_1$), anti-MASC-1 (Miltenyi[TM], clone W8-B2, IgG$_1$), anti-CD273 (B7-DC or PD-L2, eBioscience[TM], clone MIH18, IgG$_1$), anti-CD274 (B7-H1 or PD-L1, eBioscience[TM], clone MIH1, IgG$_1$), anti-HLA–ABC (BD PharMingen[TM], clone G46–2.6, IgG$_1$), anti-HLA-DR (BD PharMingen[TM], clone G46–6, IgG$_{2a}$). Phycoerythrin (PE)-conjugated polyclonal goat anti-human IgG (Fc gamma-specific)(eBioscience[TM]).

For cell count determination of CD3^{+} T cells after suppressive experiment of T cell proliferation stimulated by PHA-L, the following mouse antibodies were used: PE-conjugated anti-CD4 (BD Bioscience, clone SK3, IgG$_1$) and APC-conjugated anti-CD8 (Beckman Coulter, clone B9.11, IgG$_1$).

For Annexin V binding assay and cell count determination of CD3^{+} T cells, the following reagents and antibodies were used: Annexin V-PE (BD PharMingen[TM]), PerCP-Cy5.5-conjugated anti-CD4 (BD PharMingen[TM], clone RPA-T4, IgG$_1$), and APC-conjugated anti-CD8 (Beckman Coulter, clone B9.11, IgG$_1$).

The following color- and isotype-matched control antibodies were used to confirm the staining specificities: PE-

conjugated mouse IgG$_1$ (BD BioScience, clone X40), PE-conjugated mouse IgG$_{2a}$ (BD BioScience, clone X39), APC-conjugated mouse IgG$_{1\kappa}$ (BD PharMingen, clone MOPC-21), PerCP-Cy5.5-conjugated mouse IgG$_1$ (BD BioScience, clone X40).

Infant foreskin fibroblast cultures, carcinoma-associated fibroblasts and flow cytometry analysis

The infant FFs (14 donors with a range of ages from 18 months to 5 years) were provided by "*Banque de tissus et cellules des Hospices Civils de Lyon.*" Fibroblasts were expanded up to 3–5 passages in D-MEM medium supplemented with 10% FCS, 20 μg/mL Gentamicin, 100 U/mL Penicillin, and 100 μg/mL Streptomycin (cD-MEM medium). All FFs came from surgical residues and were used in accordance with French ethical and legal regulations. Fresh tumors from patients diagnosed with primary breast carcinoma were obtained before any treatment from the Center Léon Bérard (CLB) tissue bank after patient informed consent. The study was reviewed and approved by the Institutional Review Board of CLB. After washing with D-MEM/F-12 medium supplemented with antibiotics, the connective tissue was cut into small pieces (1 mm × 1 mm × 1 mm) that were let stick onto the bottom surface of Petri dishes for 20–30 min, then the tissue pieces were gently covered with culture medium (D-MEM/F-12 supplemented with 10% FCS, 20 μg/mL Gentamicin, 100 U/mL Penicillin, and 100 μg/mL Streptomycin (cD-MEM/F-12 medium) and incubated at 37°C, in a 5% CO$_2$ incubator. The culture medium, cD-MEM/F-12 medium, was changed every 3–4 d. When the spindle-shaped fibroblasts/myofibroblasts (Carcinoma-Associated Fibroblasts, CAFs) fully covered the Petri dishes, cells were gathered through trypsinization and expanded up to 2–3 passages. Irradiation of FFs and CAFs was performed at 30 Gray (Gy) and both fibroblast populations were subsequently cryopreserved at -80°C in a solution containing 10% DMSO and 90% FCS at a concentration of 1–3 × 10^6 cells/mL. γ-CAFs were seeded in cD-MEM/F-12 medium for phenotype determination and co-cultures with T cells. For phenotype determination, γ-FFs were seeded in cD-MEM medium at different concentrations (from 7 × 10^3/cm^2 to 140 × 10^3/cm^2) and for different time points (1 d, 4 d, and 14 d, without changing the medium) depending on the experiment conditions. Fibroblasts were trypsinized and then assayed by flow cytometry. Fibroblasts were resuspended in the labeling buffer (HBSS solution supplemented with 5% FCS, and 10 mM Hepes) (50,000 fibroblasts/50 μL) and further incubated for 20 min on ice with isotypic control or specific PE-conjugated monoclonal antibodies: anti-CD34, anti-CD45, anti-CD73, anti-CD90, anti-CD105, anti-CD146, anti-MASC-1, anti-CD273, anti-CD274, anti-HLA–ABC, and anti-HLA–DR. Then fibroblasts were washed and resuspended in 300 μL of labeling buffer containing 2 μg/mL DAPI and then further analyzed by flow cytometry. For binding of PD-1-Fc fusion protein, fibroblasts were pre-incubated with 5 μg/mL PD-1-Fc fusion protein on ice for 20 min, then washed and incubated with PE-conjugated goat anti-human IgG (Fc gamma-specific) on ice for 20 min. Then labeled fibroblasts were resuspended in 300 μL of labeling buffer containing 2 μg/mL DAPI and further analyzed by flow

cytometry. At least 30,000 total events were acquired by Cyan^{TM} ADP (Beckman Coulter) and analyzed on FlowJo^{TM} software (version 7.5.5.).

For blocking experiments, an incubation step, in presence of anti-PD-L2 mAb in a concentration range between 10 and 50 μg/mL in a PD-L1 mAb solution (50 μg/mL) was performed on ice for 20 min before PD-1-Fc fusion protein binding.

For cleaving experiments by exogenous enzymes (collagenase (CLSPA), Dispase II$^®$ and, Thermolysin), γ-FFs were seeded in cDMEM medium at the concentration of 7 × 10^3/cm^2 for 1 d, then were trypsinized and resuspended in DMEM medium without FCS and in presence of different concentrations of exogenous enzymes (CLSPA, concentration range from 500 U to 1,000 U/mL, Dispase II$^®$, concentration range from 0.25 U to 2 U/mL, and Thermolysin, concentration range from 50 to 200 μg/mL) at 37°C for 1h. Then γ-FFs were washed and resuspended in the labeling buffer (HBSS solution supplemented with 5% FCS, and 10 mM Hepes) for CD273 and CD274 expression and PD-1-Fc binding as mentioned above and further analyzed by flow cytometry.

For incubating γ-FFs with MMP inhibitors, γ-FFs were seeded at a concentration of 35 × 10^3 cells/cm^2 in P6 plates in cDMEM medium then were incubated on day 1 in presence or not of six MMP inhibitors tested at two concentrations (10 and 12 μg/mL CL82198, 0.5 and 1 μg/mL actinonin, 2 and 5 μM SB3CT, 10 and 20 μM NNGH, 10 and 20 μM Z-Pro-Leu-Gly-NHOH, 5 and 10 μM GM6001) and maintained in culture for 4 d at 37°C without medium change. Then γ-FFs were trypsinized on day 1 (control) and on day 4 (γ-FFs cultured in presence or not of MMP inhibitors) and resuspended in the labeling buffer (HBSS solution supplemented with 5% FCS, and 10 mM Hepes) for CD273, CD274 expression analysis by flow cytometry. The PD-L1/PD-L2 expression recovery (%) was expressed as following.

Ratio (%) = difference between the percentage of PD-1 ligand-positive cells incubated in presence of MMP inhibitors on day 4 and the percentage of PD-1 ligand-positive cells in absence of MMP inhibitors on day 4 ÷ difference between the percentage of PD-1 ligand-positive cells in absence of MMP inhibitors on day 1 and the percentage of PD-1 ligand-positive cells in absence of MMP inhibitors on day 4 × 100.

For cleaving experiments by recombinant human MMP-9 and MMP-13, the proforms of recombinant human MMPs were activated in TCNB (100 mM Tris, 10 mM CaCl$_2$, 150 mM NaCl, 0.05% (w/v) Brij-35, pH 8.0) in presence of p-aminophenylmercuric acetate (final concentration 0.5 mM APMA), at 37°C and 4 h for the pro-form of MMP-13 and 24 h for the pro-form of MMP-9. For cleaving experiments in suspension, γ-FFs were seeded in cDMEM medium at the concentration of 7 × 10^3/cm^2 for 2 d in presence of 100 ng/mL TNFα, then were trypsinized and fixed with 2% paraformaldehyde (PFA) in PBS (1X) for 15 min, washed for 30 min in PBS, and incubated at 37°C in presence of APMA-activated MMP-9 (200 ng/mL) and APMA-activated MMP-13 (200ng/mL) in 1% FCS culture medium (DMEM) without antibiotics. γ-FFs were then washed and resuspended in the labeling buffer (HBSS solution supplemented with 5% FCS, and 10 mM Hepes) for CD273 and CD274

expression and PD-1-Fc binding as mentioned above and further analyzed by flow cytometry.

For cleaving experiments in 96-well plates (half area), γ-FFs were seeded in cDMEM medium in triplicate at a concentration of 2,500 and 5,000 cells/well for 2 d, then washed with 1% FCS culture medium without antibiotics and incubated at 37°C for 24 h, in presence or not of APMA-activated MMP-9 (200 ng/mL) and APMA-activated MMP-13 (200 ng/mL). γ-FFs were then washed and processed for experimental procedure of the Annexin V-binding assay on T cells (as described below).

Monocyte-derived dendritic cell generation and incubation with collagenase, Dispase II®, Thermolysin, MMP-9, and MMP-13

Mo-DCs were *in vitro* generated from purified blood monocytes in presence of GM-CSF (50 ng/mL) + IL-4 (50 ng/mL) for 6 d then, activated or not for 1 additional day with *Escherichia Coli* lipopolysaccharide (100 ng/mL LPS). Mo-DCs were fixed with 2% PFA and resuspended in cRPMI1640 medium (RPMI Medium 1640, GlutaMAX™, 25 mM Hepes supplemented with 10% FCS, 20 μg/mL Gentamicin, 100 U/mL Penicillin, and 100 μg/mL Streptomycin).

For cleaving experiments by exogenous enzymes (collagenase (CLSPA), Dispase II® and, Thermolysin), Mo-DCs were resuspended in RPMI1640 medium without FCS and in presence of different concentrations of exogenous enzymes (CLSPA, concentration range from 500 U to 1,000 U/mL, Dispase II®, concentration range from 0.25 U to 1 U/mL, and Thermolysin, concentration range from 50 to 200 μg/mL) at 37°C for 1h. Then, Mo-DCs were washed and resuspended in the labeling buffer (HBSS solution supplemented with 5% FCS, and 10 mM Hepes) for CD80, CD86, CD273, and CD274 expression and PD-1-Fc binding and further analyzed by flow cytometry. For cleaving experiments by recombinant human MMP-9 and MMP-13, the protocol was similar to that followed for γ-FFs. Briefly, PFA-pre-fixed Mo-DCs were resuspended in RPMI1640 supplemented with 1% FCS in presence or not of APMA-activated MMP-9 and APMA-activated MMP-13 at 37°C for 24 h. Then, Mo-DCs were labeled for CD80, CD86, CD273 and CD274 expression and PD-1-Fc binding, and further analyzed by flow cytometry.

Quantitation of MMP secretion by infant foreskin fibroblast cultures and carcinoma-associated fibroblasts

Quantitative determination of MMP-1, MMP-9, and MMP-13 released by γ-FFs and γ-CAFs were performed by Magnetic Luminex® Performance assay (R&D Systems). γ-FFs and γ-CAFs were plated for 4 h in D-MEM supplemented with 10% FCS and D-MEM/F-12:1/1 supplemented with 10% FCS, respectively at 37°C in a 5% CO_2 incubator. γ-FFs were incubated for 2 h at 37°C in presence of 100 ng/mL TNFα in D-MEM supplemented with 1% FCS without antibiotics while γ-CAFs were directly incubated in D-MEM/F-12:1/1 supplemented with 1% FCS without antibiotics. Both γ-FFs and γ-CAFs were maintained for 5 d in their respective medium supplemented with 1% FCS (without any medium change). Supernatants (duplicate) were analyzed with a Magnetic

Luminex® Performance Assay multiplex kit including human MMP-1, MMP-9, and MMP-13. Data were acquired on Bio-Plex™ 200 System (Bio-Rad Laboratories) and analyzed on Bio-Plex Manager (version 6.1).

Detection of senescence-associated β-galactosidase (SA-βgal) activity in 30 Gray-irradiated infant foreskin fibroblasts

The detection of individual senescent cells was based on the alkalinization of lysosomes, followed by the use of 5-dodecanoylaminofluorescein di-β-D-galactopyranoside (C_{12}FDG), a fluorogenic substrate for βgal activity.[40] Under similar seeding cell density (13×10^3/cm²) γ-FFs were maintained in culture for 1, 4, and 14 d. Positive control (induction of lysosomal alkalinization) was performed by treatment of plated γ-FFs with 100 nM bafilomycin A1 for 1 h at 37°C in a 5% CO_2 incubator. γ-FFs and bafilomycin A1-treated γ-FFs were treated (Samples and Positive controls, respectively) or not (Negative controls) with 2 mM C_{12}FDG for 1–2 h at 37°C in a 5% CO_2 incubator. After washing with PBS (1X), the cells were harvested by trypsinization and then, resuspended in 300 μL of PBS (1X) containing 2 μg/mL DAPI and further analyzed by flow cytometry. Events were acquired by Cyan™ ADP (Beckman Coulter) and analyzed on FlowJo™ software (version 7.5.5.).

RNA extraction and droplet digital PCR quantitation of PD-L1, PD-L2 and CD10 in 30 Gray-irradiated infant foreskin fibroblasts

Under similar seeding cell density (13×10^3/cm²) γ-FFs were maintained in culture for 1, 4, and 14 d and then, harvested by trypsinization. Total RNA was extracted from cell pellets using a single phenol/chloroform extraction protocol with TRIzol® Reagent (Ambion, Life technologies™) according to the manufacturer's instructions. The cDNA was generated using the SuperScript® VILO™ cDNA Synthesis kit (Invitrogen, Life technologies™) with 7 ng of total RNA according to the manufacturer's instructions. The primers and probes were designed using Primer Express® Software v3.0 (Table 1). For PD-L1, an amplicon of 54 bp was designed in the common region of the immunoglobulin variable domain (IgV)-like domain of PD-L1, and for PD-L2, an amplicon was designed in a common sequence present in the two forms of PD-L2. The ddPCR workflow was carried out as previously described.[83,84] Briefly, the PCR reaction mixture was assembled with 10 μL of a 2x ddPCR™ Supermix for Probes (No dUTP) (Bio-Rad

Table 1. Primer sets and probes used for droplet digital PCR study. All primers and probes were designed by Primer Express® Software v3.0.

CD10-f	Forward primer	CTACGGCTAAACCTGAAGATCGA
CD10-r	Reverse primer	TCTGGGCCAATGTCATCTTG
CD10	Probe	VIC-ATGATCCAATGCTTCTG-MGB
PD-L1-f	Forward primer	AAAGAATTTTGGTTGTGGATCCA
PD-L1-r	Reverse primer	AGCCCTCAGCCTGACATGTC
PD-L1	Probe	6FAM-TCACCTCTGAACATGAAC-MGB
PD-L2-f	Forward primer	AGTTTGCAAAAGGTGGAAAATGA
PD-L2-r	Reverse primer	TCCTCCAGCAAAGTGGCTCTT
PD-L2	Probe	6FAM-ACATCCCCACACCGTG-MGB

Technologies), 1 μL of each primer (900 nM final concentration) (Table 1), 1 μL of probe (250 nM final concentration) (Table 1), 1 μL of cDNA and 7 μL of water. The droplet was generated by the addition of 70 μL of droplet generation oil (Bio-Rad Technologies), to 20 μL of the PCR reaction mixture in the droplet generator cartridge (DG8[TM], Bio-Rad Technologies), and the emulsified samples were generated from a droplet generator. Droplets were then thermocycled at 95°C for 10 min, followed by 40 cycles of 95°C for 30 s, 60°C for 1 min, and a final extension for 10 min at 98°C. After PCR, the 96-well PCR plate was loaded on the Bio-Rad QX200[TM] Droplet Reader (Bio-Rad Technologies). Analysis of the ddPCR data was performed with QuantaSoft[TM] analysis software (Bio-Rad Technologies). The ddPCR data were analyzed when more than 15,000 droplets/well were read. GAPDH was used as the reference gene both in Reverse Transcription validation and ddPCR data normalization. All transcript concentrations are given in copy number/μL.

Human CD3^{+} T cell isolation

Healthy human blood obtained anonymously from the "*Etablissement Francais du Sang, EFS*" (Gerland-Lyon, France) after donor informed consent was collected in sterile bags containing CTAD. Peripheral blood mononuclear cells (PBMC) were isolated by gradient centrifugation on lymphocyte separation medium (density 1.077g/L). Cells were washed twice in phosphate-buffered saline (PBS) (1X) and suspended in PBS (1X) supplemented with 5% FCS. PBMC were depleted from monocytes, NK cells, MDCs and plasmacytoid DCs (pDCs) by gradient centrifugation on Percoll®Plus and resuspended in PBS (1X) supplemented with 2% FCS. For depletion experiments, different cell subsets (monocytes, MDCs, pDCs, NK cells, and B cells) were specifically depleted from PBMCs using positive selection including anti-human mouse mAbs: anti-CD11b (clone Bear1, IgG$_{1\kappa}$), anti-CD14 (clone RM052, IgG$_{2a\kappa}$), anti-CD16 (clone 3G8, IgG$_1$), anti-CD19 (clone J3–119, IgG$_1$), anti-CD35 (clone J3D3, IgG$_{1\kappa}$), anti-CD56 (clone C218, IgG$_{1\kappa}$) and anti-CD235a (clone 11E4B-7–6, IgG$_1$) from Beckman Coulter® and magnetic beads (goat anti-mouse (GAM) IgG dynabeads, Dynal® by Invitrogen). The absence of remaining positive cells in the depleted fraction was confirmed by flow cytometry. The depleted fraction of untouched double CD3^{+}/CD4^{+} T cells: CD3^{+}/CD8^{+} T cells (purity 95–98%) was resuspended in complete RPMI Medium 1640 with GlutaMAX[TM] and 25 mM Hepes supplemented with 10% FCS, 20 μg/mL Gentamicin, 100 U/mL Penicillin, and 100 μg/mL Streptomycin (cRPMI medium). CD3^{+} T cells were subsequently cryopreserved in liquid nitrogen (−196°C) in a solution containing 10% DMSO and 90% FCS at a concentration of 50–60 × 10^{6} cells/mL.

Co-culture of CFSE-stained CD3^{+} T cells on 30 Gy-irradiated infant foreskin fibroblasts

Cryopreserved γ-FFs were thawed and then seeded in 96-well black plates (half area, Greiner bio-one® provided by Dominique Dutscher) in triplicate at a concentration of 1,250 or 2,500 or 5,000 cells/well, 1 day prior their incubation with or without 100 ng/mL TNFα + 100 ng/mL IL-1α or 100 ng/mL

IFNγ + 100 ng/mL TNFα + 100 ng/mL IL-1α. The γ-FFs were cultured for 48 h and washed twice before addition of CFSE-stained T cells.

T cell proliferation was measured using CFSE dilution assay and immunophenotyped (CD4^{+} and CD8^{+} phenotype) by T cell counting. Cryopreserved CD3^{+} T cells were thawed, washed twice in cold PBS (1X) and resuspended at 5 × 10^{6} total cells/mL in PBS (1X) with 0.1% Bovine Serum Albumin (BSA). CFSE was added at a final concentration of 1 μM and incubated at RT for 10 min. Staining was then quenched by the addition of at least two volumes of FCS. T cells were washed three times and then resuspended at 1 × 10^{6} T cells/mL in cRPMI supplemented with 50 U/mL IL-2 and 5 ng/mL IL-7. One hundred thousand CFSE-stained T cells were added to wells seeded or not with γ-FFs which were stimulated or not with cytokines and incubated at 37°C in a 5% CO$_2$ incubator. After 4 h of co-culture between γ-FFs and T cells, 0.5 μg/mL of PHA-L was added or not to each well. Then, plates were incubated at 37°C in a 5% CO$_2$ incubator for 7 d CFSE-stained cells were harvested, immunophenotyped with PE-conjugated anti-CD4 mAb and APC-conjugated anti-CD8 mAb on ice for 20 min. Then, T cells were washed, resuspended in 300 μL of labeling buffer containing 0.6 μg DAPI and then further analyzed by flow cytometry. For T cell count determination, 20,000 inert polystyrene beads (size 15μm, PolyScience[TM]) were added. At least 15,000 bead events were acquired by Cyan[TM] ADP (Beckman Coulter). Data were analyzed on FlowJo[TM] software (version 7.5.5.).

In blocking experiments, cryopreserved γ-FFs were thawed and were then seeded in 96-well black plates (half area) in triplicate at a concentration of 2,500 or 5,000 cells/well, then incubated with or without 100 μg/mL TNFα for 48 h. Four hours prior the addition of 1-day cultured T cells, γ-FFs stimulated or not with TNFα were incubated either with a mixed PD-L1 mAb (clone 29E23A3)/PD-L2 mAb (clone 24F10C12) solution or with a mixed mouse IgG$_{2a}$/IgG$_{2b}$ solution at the concentration of 50 μg/mL. Then, 100,000 T cells were added and incubated for 4 h with γ-FFs treated or not with TNFα. Then, 0.5 μg/mL of PHA-L was added or not to each well. Plates were further incubated at 37°C in a 5% CO$_2$ incubator for 7 d. T cells were harvested from each well and immunophenotyped as described above. As previously, data were analyzed on FlowJo[TM] software (version 7.5.5.).

Annexin V-binding assay on CD3^{+} T cells cultured on 30 Gy-irradiated infant foreskin fibroblasts

To confirm the induction of apoptosis on CD3^{+} T cells cultured on 30 Gy-irradiated infant FFs in presence of PHA-L, the binding of Annexin V to externalized PS on the outer cellular surface was assessed.

At first, cryopreserved γ-irradiated FFs were thawed and seeded in 96-well plates (Costar) in triplicate at a concentration of 10,000 cells/well, then incubated with or without 100 μg/mL TNFα for 48 h. After washing, 1-day cultured T cells were added to each well with or without γ-FFs treated or not with TNFα. After 3 h of incubation, 0.25 μg/mL of PHA-L was added to each well. Plates were further incubated at 37°C in a 5% CO$_2$ incubator for 17 h. T cells were harvested from each

well and immunophenotyped on ice with PerCP-Cy5.5-conjugated anti-CD4 mAb and APC-conjugated anti-CD8 mAb on ice for 20 min. Then, T cells were washed, once in PBS (1X) and once, in the Annexin V binding buffer (10 mM Hepes, 140 mM NaCl, 2.5 mM $CaCl_2$, pH 7.4). Subsequently, cells were resuspended and incubated in Annexin V binding buffer with Annexin V-PE (1:25) at RT for 15 min. 50 μL of T cells were harvested in 250 μL of Annexin V binding buffer containing 0.6 μg of DAPI and, further analyzed by flow cytometry. Total T cell events were acquired by Cyan^{TM} ADP (Beckman Coulter). Data were analyzed on FlowJo^{TM} software. Viable cells were identified as DAPI$^-$ cells, and cells in early stage of apoptosis as DAPI-/Annexin V$^+$ T cells.

In blocking experiments, cryopreserved γ-FFs were thawed and, then were seeded in 96-well plates (Costar) in triplicate at a concentration of 5,000 and 10,000 cells/well. Four hours prior the addition of 1 day-cultured T cells (200,000 T cells), γ-FFs were incubated either with a mixed PD-L1 mAb (clone 29E23A3)/PD-L2 mAb (clone 24F10C12) solution or with a mixed mouse IgG_{2a}/IgG_{2b} solution at the concentration of 50 μg/mL at 37°C in a 5% CO_2 incubator. As described above, after 3 h of co-incubation γ-FFs:T cells, 0.25 μg/mL of PHA-L was added to each well. Plates were further incubated at 37°C in a 5% CO2 incubator for 17 h. T cells were harvested from each well and immunophenotyped as previously. Viable T cells and early apoptotic T cells were distinguished by analysis on FlowJo^{TM} software. Because of spontaneous apoptosis of PHA-stimulated T cells, the data are expressed as the differences between the percentage of early apoptotic T cells cultured in presence of γ-FFs and the percentage of early apoptotic T cells kept alone.

Statistical analysis

Statistical analysis was performed with the GraphPad Prism version 6.0 (GraphPad software). Significance was estimated by nonparametric Wilcoxon–Mann Whitney test. Differences were considered significant at $p < 0.05$.

Disclosure of potential conflicts of interest

No potential conflicts of interest were disclosed.

Acknowledgments

Funding

References

1. Bernardo ME, Fibbe WE. Mesenchymal stromal cells: sensors and switchers of inflammation. Cell Stem Cell 2013; 13:392-402; PMID:24094322; http://dx.doi.org/10.1016/j.stem.2013.09.006

2. Frenette PS, Pinho S, Lucas D, Scheiermann C. Mesenchymal stem cell: keystone of the hematopoietic stem cell niche and a stepping-stone for regenerative medicine. Annu Rev Immunol 2013; 31:285-316; PMID:23298209; http://dx.doi.org/10.1146/annurev-immunol-032712-095919

3. Le BK, Mougiakakos D. Multipotent mesenchymal stromal cells and the innate immune system. Nat Rev Immunol 2012; 12:383-96; PMID:22531326; http://dx.doi.org/10.1038/nri3209

4. Chang HY, Chi JT, Dudoit S, Bondre C, van de Rijn M, Botstein D, Brown PO. Diversity, topographic differentiation, and positional memory in human fibroblasts. Proc Natl Acad Sci U S A 2002; 99:12877-82; PMID:12297622; http://dx.doi.org/10.1073/pnas.162488599

5. Haniffa MA, Wang XN, Holtick U, Rae M, Isaacs JD, Dickinson AM, Hilkens CM, Collin MP. Adult human fibroblasts are potent immuno-regulatory cells and functionally equivalent to mesenchymal stem cells. J Immunol 2007; 179:1595-604; PMID:17641026; http://dx.doi.org/10.4049/jimmunol.179.3.1595

6. Cappellesso-Fleury S, Puissant-Lubrano B, Apoil PA, Titeux M, Winterton P, Casteilla L, Bourin P, Blancher A. Human fibroblasts share immunosuppressive properties with bone marrow mesenchymal stem cells. J Clin Immunol 2010; 30:607-19; PMID:20405178; http://dx.doi.org/10.1007/s10875-010-9415-4

7. Jones S, Horwood N, Cope A, Dazzi F. The antiproliferative effect of mesenchymal stem cells is a fundamental property shared by all stromal cells. J Immunol 2007; 179:2824-31; PMID:17709496; http://dx.doi.org/10.4049/jimmunol.179.5.2824

8. Rasanen K, Vaheri A. Activation of fibroblasts in cancer stroma. Exp Cell Res 2010; 316:2713-22; PMID:20451516; http://dx.doi.org/10.1016/j.yexcr.2010.04.032

9. Buckley CD, Pilling D, Lord JM, Akbar AN, Scheel-Toellner D, Salmon M. Fibroblasts regulate the switch from acute resolving to chronic persistent inflammation. Trends Immunol 2001; 22:199-204; PMID:11274925; http://dx.doi.org/10.1016/S1471-4906(01)01863-4

10. Kalluri R, Zeisberg M. Fibroblasts in cancer. Nat Rev Cancer 2006; 6:392-401; PMID:16572188; http://dx.doi.org/10.1038/nrc1877

11. Nazareth MR, Broderick L, Simpson-Abelson MR, Kelleher RJ, Jr., Yokota SJ, Bankert RB. Characterization of human lung tumor-associated fibroblasts and their ability to modulate the activation of tumor-associated T cells. J Immunol 2007; 178:5552-62; PMID:17442937; http://dx.doi.org/10.4049/jimmunol.178.9.5552

12. Keir ME, Butte MJ, Freeman GJ, Sharpe AH. PD-1 and its ligands in tolerance and immunity. Annu Rev Immunol 2008; 26:677-704; PMID:18173375; http://dx.doi.org/10.1146/annurev.immunol.26.021607.090331

13. Chemnitz JM, Parry RV, Nichols KE, June CH, Riley JL. SHP-1 and SHP-2 associate with immunoreceptor tyrosine-based switch motif of programmed death 1 upon primary human T cell stimulation, but only receptor ligation prevents T cell activation. J Immunol 2004; 173:945-54; PMID:15240681; http://dx.doi.org/10.4049/jimmunol.173.2.945

14. Gianchecchi E, Delfino DV, Fierabracci A. Recent insights into the role of the PD-1/PD-L1 pathway in immunological tolerance and autoimmunity. Autoimmun Rev 2013; 12:1091-100; PMID:23792703; http://dx.doi.org/10.1016/j.autrev.2013.05.003

15. Pardoll DM. The blockade of immune checkpoints in cancer immunotherapy. Nat Rev Cancer 2012; 12:252-64; PMID:22437870; http://dx.doi.org/10.1038/nrc3239

16. Hamid O, Robert C, Daud A, Hodi FS, Hwu WJ, Kefford R, Wolchok JD, Hersey P, Joseph RW, Weber JS et al. Safety and tumor responses with lambrolizumab (anti-PD-1) in melanoma. N Engl J Med 2013; 369:134-44; PMID:23724846; http://dx.doi.org/10.1056/NEJMoa1305133

17. Robert C, Karaszewska B, Schachter J, Rutkowski P, Mackiewicz A, Stroiakovski D, Lichinitser M, Dummer R, Grange F, Mortier L et al. Improved overall survival in melanoma with combined dabrafenib and trametinib. N Engl J Med 2015; 372:30-9; PMID:25399551; http://dx.doi.org/10.1056/NEJMoa1412690

18. Topalian SL, Hodi FS, Brahmer JR, Gettinger SN, Smith DC, McDermott DF, Powderly JD, Carvajal RD, Sosman JA, Atkins MB et al. Safety, activity, and immune correlates of anti-PD-1 antibody in cancer. N Engl J Med 2012; 366:2443-54; PMID:22658127; http://dx.doi.org/10.1056/NEJMoa1200690

19. Tumeh PC, Harview CL, Yearley JH, Shintaku IP, Taylor EJ, Robert L, Chmielowski B, Spasic M, Henry G, Ciobanu V et al. PD-1 blockade induces responses by inhibiting adaptive immune resistance. Nature 2014; 515:568-71; PMID:25428505; http://dx.doi.org/10.1038/nature13954

20. Herbst RS, Soria JC, Kowanetz M, Fine GD, Hamid O, Gordon MS, Sosman JA, McDermott DF, Powderly JD, Gettinger SN et al. Predictive correlates of response to the anti-PD-L1 antibody MPDL3280A in cancer patients. Nature 2014; 515:563-7; PMID:25428504; http://dx.doi.org/10.1038/nature14011

21. Powles T, Eder JP, Fine GD, Braiteh FS, Loriot Y, Cruz C, Bellmunt J, Burris HA, Petrylak DP, Teng SL et al. MPDL3280A (anti-PD-L1) treatment leads to clinical activity in metastatic bladder cancer. Nature 2014; 515:558-62; PMID:25428503; http://dx.doi.org/10.1038/nature13904

22. Taube JM, Klein A, Brahmer JR, Xu H, Pan X, Kim JH, Chen L, Pardoll DM, Topalian SL, Anders RA. Association of PD-1, PD-1 ligands, and other features of the tumor immune microenvironment with response to anti-PD-1 therapy. Clin Cancer Res 2014; 20:5064-74; PMID:24714771; http://dx.doi.org/10.1158/1078-0432.CCR-13-3271

23. Eppihimer MJ, Gunn J, Freeman GJ, Greenfield EA, Chernova T, Erickson J, Leonard JP. Expression and regulation of the PD-L1 immunoinhibitory molecule on microvascular endothelial cells. Microcirculation 2002; 9:133-45; PMID:11932780; http://dx.doi.org/10.1080/713774061

24. Tewalt EF, Cohen JN, Rouhani SJ, Guidi CJ, Qiao H, Fahl SP, Conaway MR, Bender TP, Tung KS, Vella AT et al. Lymphatic endothelial cells induce tolerance via PD-L1 and lack of costimulation leading to high-level PD-1 expression on CD8 T cells. Blood 2012; 120:4772-82; PMID:22993390; http://dx.doi.org/10.1182/blood-2012-04-427013

25. Keir ME, Liang SC, Guleria I, Latchman YE, Qipo A, Albacker LA, Koulmanda M, Freeman GJ, Sayegh MH, Sharpe AH. Tissue expression of PD-L1 mediates peripheral T cell tolerance. J Exp Med 2006; 203:883-95; PMID:16606670; http://dx.doi.org/10.1084/jem.20051776

26. Youngnak-Piboonratanakit P, Tsushima F, Otsuki N, Igarashi H, Machida U, Iwai H, Takahashi Y, Omura K, Yokozeki H, Azuma M. The expression of B7-H1 on keratinocytes in chronic inflammatory mucocutaneous disease and its regulatory role. Immunol Lett 2004; 94:215-22; PMID:15275969; http://dx.doi.org/10.1016/j.imlet.2004.05.007

27. Latchman Y, Wood CR, Chernova T, Chaudhary D, Borde M, Chernova I, Iwai Y, Long AJ, Brown JA, Nunes R et al. PD-L2 is a second ligand for PD-1 and inhibits T cell activation. Nat Immunol 2001; 2:261-8; PMID:11224527; http://dx.doi.org/10.1038/85330

28. Rozali EN, Hato SV, Robinson BW, Lake RA, Lesterhuis WJ. Programmed death ligand 2 in cancer-induced immune suppression. Clin Dev Immunol 2012; 2012:656340; PMID:22611421; http://dx.doi.org/10.1155/2012/656340

29. Youngnak P, Kozono Y, Kozono H, Iwai H, Otsuki N, Jin H, Omura K, Yagita H, Pardoll DM, Chen L et al. Differential binding properties of B7-H1 and B7-DC to programmed death-1. Biochem Biophys Res Commun 2003; 307:672-7; PMID:12893276; http://dx.doi.org/10.1016/S0006-291X(03)01257-9

30. Augello A, Tasso R, Negrini SM, Amateis A, Indiveri F, Cancedda R, Pennesi G. Bone marrow mesenchymal progenitor cells inhibit lymphocyte proliferation by activation of the programmed death 1 pathway. Eur J Immunol 2005; 35:1482-90; PMID:15827960; http://dx.doi.org/10.1002/eji.200425405

31. Lee SK, Seo SH, Kim BS, Kim CD, Lee JH, Kang JS, Maeng PJ, Lim JS. IFN-gamma regulates the expression of B7-H1 in dermal fibroblast cells. J Dermatol Sci 2005; 40:95-103; PMID:16085391; http://dx.doi.org/10.1016/j.jdermsci.2005.06.008

32. Pinchuk IV, Saada JI, Beswick EJ, Boya G, Qiu SM, Mifflin RC, Raju GS, Reyes VE, Powell DW. PD-1 ligand expression by human colonic myofibroblasts/fibroblasts regulates CD4+ T-cell activity. Gastroenterol 2008; 135:1228-37, 1237; PMID:18760278; http://dx.doi.org/10.1053/j.gastro.2008.07.016

33. Wang X, Marr AK, Breitkopf T, Leung G, Hao J, Wang E, Kwong N, Akhoundsadegh N, Chen L, Mui A et al. Hair follicle mesenchyme-associated PD-L1 regulates T-cell activation induced apoptosis: a potential mechanism of immune privilege. J Invest Dermatol 2014; 134:736-45; PMID:24005055; http://dx.doi.org/10.1038/jid.2013.368

34. Stagg J, Pommey S, Eliopoulos N, Galipeau J. Interferon-gamma-stimulated marrow stromal cells: a new type of nonhematopoietic antigen-presenting cell. Blood 2006; 107:2570-7; PMID:16293599; http://dx.doi.org/10.1182/blood-2005-07-2793

35. de Andrade AV, Riewaldt J, Wehner R, Schmitz M, Odendahl M, Bornhauser M, Tonn T. Gamma irradiation preserves immuno-suppressive potential and inhibits clonogenic capacity of human bone marrow-derived mesenchymal stromal cells. J Cell Mol Med 2014; 18:1184-93; PMID:24655362; http://dx.doi.org/10.1111/jcmm.12264

36. Fekete N, Erle A, Amann EM, Furst D, Rojewski MT, Langonne A, Sensebe L, Schrezenmeier H, Schmidtke-Schrezenmeier G. Effect of High-Dose Irradiation on Human Bone-Marrow-Derived Mesenchymal Stromal Cells. Tissue Eng Part C Methods 2015; 21:212–22; PMID:24918644; http://dx.doi.org/10.1089/ten.TEC.2013.0766

37. Ghiotto M, Gauthier L, Serriari N, Pastor S, Truneh A, Nunes JA, Olive D. PD-L1 and PD-L2 differ in their molecular mechanisms of interaction with PD-1. Int Immunol 2010; 22:651-60; PMID:20587542; http://dx.doi.org/10.1093/intimm/dxq049

38. Lemons JM, Feng XJ, Bennett BD, Legesse-Miller A, Johnson EL, Raitman I, Pollina EA, Rabitz HA, Rabinowitz JD, Coller HA. Quiescent fibroblasts exhibit high metabolic activity. PLoS Biol 2010; 8:e1000514; PMID:21049082; http://dx.doi.org/10.1371/journal.pbio.1000514

39. Papadopoulou A, Kletsas D. Human lung fibroblasts prematurely senescent after exposure to ionizing radiation enhance the growth of malignant lung epithelial cells in vitro and in vivo. Int J Oncol 2011; 39:989-99; PMID:21814715; http://dx.doi.org/10.3892/ijo.2011.1132

40. Debacq-Chainiaux F, Erusalimsky JD, Campisi J, Toussaint O. Protocols to detect senescence-associated β-galactosidase (SA-betagal) activity, a biomarker of senescent cells in culture and in vivo. Nat Protoc 2009; 4:1798-806; PMID:20010931; http://dx.doi.org/10.1038/nprot.2009.191

41. Khokha R, Murthy A, Weiss A. Metalloproteinases and their natural inhibitors in inflammation and immunity. Nat Rev Immunol 2013; 13:649-65; PMID:23969736; http://dx.doi.org/10.1038/nri3499

42. Merdad A, Karim S, Schulten HJ, Dallol A, Buhmeida A, Al-Thubaity F, Gari MA, Chaudhary AG, Abuzenadah AM, Al-Qahtani MH. Expression of matrix metalloproteinases (MMPs) in primary human breast cancer: MMP-9 as a potential biomarker for cancer invasion and metastasis. Anticancer Res 2014; 34:1355-66; PMID:24596383

43. Toriseva M, Laato M, Carpen O, Ruohonen ST, Savontaus E, Inada M, Krane SM, Kahari VM. MMP-13 regulates growth of wound granulation tissue and modulates gene expression signatures involved in inflammation, proteolysis, and cell viability. PLoS One 2012; 7:e42596; PMID:22880047; http://dx.doi.org/10.1371/journal.pone.0042596

44. Dai S, Jia R, Zhang X, Fang Q, Huang L. The PD-1/PD-Ls pathway and autoimmune diseases. Cell Immunol 2014; 290:72-9; PMID:24908630; http://dx.doi.org/10.1016/j.cellimm.2014.05.006

45. Gu YZ, Xue Q, Chen YJ, Yu GH, Qing MD, Shen Y, Wang MY, Shi Q, Zhang XG. Different roles of PD-L1 and FasL in immunomodulation mediated by human placenta-derived mesenchymal stem cells. Hum Immunol 2013; 74:267-76; PMID:23261407; http://dx.doi.org/10.1016/j.humimm.2012.12.011

46. English K, Barry FP, Mahon BP. Murine mesenchymal stem cells suppress dendritic cell migration, maturation and antigen presentation. Immunol Lett 2008; 115:50-8; PMID:18022251; http://dx.doi.org/10.1016/j.imlet.2007.10.002

47. Chang CJ, Yen ML, Chen YC, Chien CC, Huang HI, Bai CH, Yen BL. Placenta-derived multipotent cells exhibit immunosuppressive properties that are enhanced in the presence of interferon-gamma. Stem Cells 2006; 24:2466-77; PMID:17071860; http://dx.doi.org/10.1634/stemcells.2006-0071

48. Schreiner B, Mitsdoerffer M, Kieseier BC, Chen L, Hartung HP, Weller M, Wiendl H. Interferon-β enhances monocyte and dendritic cell expression of B7-H1 (PD-L1), a strong inhibitor of autologous T-cell activation: relevance for the immune modulatory effect in multiple sclerosis. J Neuroimmunol 2004; 155:172-82; PMID:15342209; http://dx.doi.org/10.1016/j.jneuroim.2004.06.013

49. Akbay EA, Koyama S, Carretero J, Altabef A, Tchaicha JH, Christensen CL, Mikse OR, Cherniack AD, Beauchamp EM, Pugh TJ et al. Activation of the PD-1 pathway contributes to immune escape in EGFR-driven lung tumors. Cancer Discov 2013; 3:1355-63; PMID:24078774; http://dx.doi.org/10.1158/2159-8290.CD-13-0310

50. Xu W, Jiang H, Gao J, Zhao Y. The upregulation of immune checkpoint ligand PD-L1 in tumour microenvironment. Scand J Immunol 2014; 80:71-2; PMID:24684652; http://dx.doi.org/10.1111/sji.12177

51. Rodig N, Ryan T, Allen JA, Pang H, Grabie N, Chernova T, Greenfield EA, Liang SC, Sharpe AH, Lichtman AH et al. Endothelial expression of PD-L1 and PD-L2 down-regulates CD8+ T cell activation and cytolysis. Eur J Immunol 2003; 33:3117-26; PMID:14579280; http://dx.doi.org/10.1002/eji.200324270

52. Stanciu LA, Bellettato CM, Laza-Stanca V, Coyle AJ, Papi A, Johnston SL. Expression of programmed death-1 ligand (PD-L) 1, PD-L2, B7-H3, and inducible costimulator ligand on human respiratory tract epithelial cells and regulation by respiratory syncytial virus and type 1 and 2 cytokines. J Infect Dis 2006; 193:404-12; PMID:16388488; http://dx.doi.org/10.1086/499275

53. Muhlbauer M, Fleck M, Schutz C, Weiss T, Froh M, Blank C, Scholmerich J, Hellerbrand C. PD-L1 is induced in hepatocytes by viral infection and by interferon-α and -gamma and mediates T cell apoptosis. J Hepatol 2006; 45:520-8; PMID:16876901; http://dx.doi.org/10.1016/j.jhep.2006.05.007

54. Kinter AL, Godbout EJ, McNally JP, Sereti I, Roby GA, O'Shea MA, Fauci AS. The common gamma-chain cytokines IL-2, IL-7, IL-15, and IL-21 induce the expression of programmed death-1 and its ligands. J Immunol 2008; 181:6738-46; PMID:18981091; http://dx.doi.org/10.4049/jimmunol.181.10.6738

55. Lesterhuis WJ, Steer H, Lake RA. PD-L2 is predominantly expressed by Th2 cells. Mol Immunol 2011; 49:1-3; PMID:22000002; http://dx.doi.org/10.1016/j.molimm.2011.09.014

56. Curiel TJ, Wei S, Dong H, Alvarez X, Cheng P, Mottram P, Krzysiek R, Knutson KL, Daniel B, Zimmermann MC et al. Blockade of B7-H1 improves myeloid dendritic cell-mediated antitumor immunity. Nat Med 2003; 9:562-7; PMID:12704383; http://dx.doi.org/10.1038/nm863

57. Shi F, Shi M, Zeng Z, Qi RZ, Liu ZW, Zhang JY, Yang YP, Tien P, Wang FS. PD-1 and PD-L1 upregulation promotes CD8(+) T-cell apoptosis and postoperative recurrence in hepatocellular carcinoma patients. Int J Cancer 2011; 128:887-96; PMID:20473887; http://dx.doi.org/10.1002/ijc.25397

58. Benson JR, Wakefield LM, Baum M, Colletta AA. Synthesis and secretion of transforming growth factor β isoforms by primary cultures of human breast tumour fibroblasts in vitro and their modulation by tamoxifen. Br J Cancer 1996; 74:352-8; PMID:8695348; http://dx.doi.org/10.1038/bjc.1996.365

59. Ina K, Kusugami K, Kawano Y, Nishiwaki T, Wen Z, Musso A, West GA, Ohta M, Goto H, Fiocchi C. Intestinal fibroblast-derived IL-10 increases survival of mucosal T cells by inhibiting growth factor deprivation- and Fas-mediated apoptosis. J Immunol 2005; 175:2000-9; PMID:16034145; http://dx.doi.org/10.4049/jimmunol.175.3.2000

60. Pang G, Couch L, Batey R, Clancy R, Cripps A. GM-CSF, IL-1 α, IL-1 β, IL-6, IL-8, IL-10, ICAM-1 and VCAM-1 gene expression and cytokine production in human duodenal fibroblasts stimulated with lipopolysaccharide, IL-1 α and TNF-α. Clin Exp Immunol 1994; 96:437-43; PMID:8004813; http://dx.doi.org/10.1111/j.1365-2249.1994.tb06048.x

61. Rasmusson I, Ringden O, Sundberg B, Le BK. Mesenchymal stem cells inhibit lymphocyte proliferation by mitogens and alloantigens by

62. Sarkhosh K, Tredget EE, Karami A, Uludag H, Iwashina T, Kilani RT, Ghahary A. Immune cell proliferation is suppressed by the interferon-gamma-induced indoleamine 2,3-dioxygenase expression of fibroblasts populated in collagen gel (FPCG). J Cell Biochem 2003; 90:206-17; PMID:12938169; http://dx.doi.org/10.1002/jcb.10593

63. Kessenbrock K, Plaks V, Werb Z. Matrix metalloproteinases: regulators of the tumor microenvironment. Cell 2010; 141:52-67; PMID:20371345; http://dx.doi.org/10.1016/j.cell.2010.03.015

64. Toriseva MJ, Ala-aho R, Karvinen J, Baker AH, Marjomaki VS, Heino J, Kahari VM. Collagenase-3 (MMP-13) enhances remodeling of three-dimensional collagen and promotes survival of human skin fibroblasts. J Invest Dermatol 2007; 127:49-59; PMID:16917496; http://dx.doi.org/10.1038/sj.jid.5700500

65. Chen Y, Wang Q, Shi B, Xu P, Hu Z, Bai L, Zhang X. Development of a sandwich ELISA for evaluating soluble PD-L1 (CD274) in human sera of different ages as well as supernatants of PD-L1+ cell lines. Cytokine 2011; 56:231-8; PMID:21733718; http://dx.doi.org/10.1016/j.cyto.2011.06.004

66. Frigola X, Inman BA, Lohse CM, Krco CJ, Cheville JC, Thompson RH, Leibovich B, Blute ML, Dong H, Kwon ED. Identification of a soluble form of B7-H1 that retains immunosuppressive activity and is associated with aggressive renal cell carcinoma. Clin Cancer Res 2011; 17:1915-23; PMID:21355078; http://dx.doi.org/10.1158/1078-0432.CCR-10-0250

67. He XH, Liu Y, Xu LH, Zeng YY. Cloning and identification of two novel splice variants of human PD-L2. Acta Biochim Biophys Sin (Shanghai) 2004; 36:284-9; PMID:15253154; http://dx.doi.org/10.1093/abbs/36.4.284

68. Murphy G, Murthy A, Khokha R. Clipping, shedding and RIPping keep immunity on cue. Trends Immunol 2008; 29:75-82; PMID:18182322; http://dx.doi.org/10.1016/j.it.2007.10.009

69. McQuibban GA, Gong JH, Tam EM, McCulloch CA, Clark-Lewis I, Overall CM. Inflammation dampened by gelatinase A cleavage of monocyte chemoattractant protein-3. Science 2000; 289:1202-6; PMID:10947989; http://dx.doi.org/10.1126/science.289.5482.1202

70. Van den Steen PE, Wuyts A, Husson SJ, Proost P, Van DJ, Opdenakker G. Gelatinase B/MMP-9 and neutrophil collagenase/MMP-8 process the chemokines human GCP-2/CXCL6, ENA-78/CXCL5 and mouse GCP-2/LIX and modulate their physiological activities. Eur J Biochem 2003; 270:3739-49; PMID:12950257; http://dx.doi.org/10.1046/j.1432-1033.2003.03760.x

71. Van den Steen PE, Husson SJ, Proost P, Van DJ, Opdenakker G. Carboxyterminal cleavage of the chemokines MIG and IP-10 by gelatinase B and neutrophil collagenase. Biochem Biophys Res Commun 2003; 310:889-96; PMID:14550288; http://dx.doi.org/10.1016/j.bbrc.2003.09.098

72. Black RA, Rauch CT, Kozlosky CJ, Peschon JJ, Slack JL, Wolfson MF, Castner BJ, Stocking KL, Reddy P, Srinivasan S et al. A metalloproteinase disintegrin that releases tumour-necrosis factor-α from cells. Nature 1997; 385:729-33; PMID:9034190; http://dx.doi.org/10.1038/385729a0

73. Weskamp G, Ford JW, Sturgill J, Martin S, Docherty AJ, Swendeman S, Broadway N, Hartmann D, Saftig P, Umland S et al. ADAM10 is a principal 'sheddase' of the low-affinity immunoglobulin E receptor CD23. Nat Immunol 2006; 7:1293-8; PMID:17072319; http://dx.doi.org/10.1038/ni1399

74. Logue EC, Bakkour S, Murphy MM, Nolla H, Sha WC. ICOS-induced B7h shedding on B cells is inhibited by TLR7/8 and TLR9. J Immunol 2006; 177:2356-64; PMID:16887997; http://dx.doi.org/10.4049/jimmunol.177.4.2356

75. Sun J, Chen LJ, Zhang GB, Jiang JT, Zhu M, Tan Y, Wang HT, Lu BF, Zhang XG. Clinical significance and regulation of the costimulatory molecule B7-H3 in human colorectal carcinoma. Cancer Immunol Immunother 2010; 59:1163-71; PMID:20333377; http://dx.doi.org/10.1007/s00262-010-0841-1

76. Zhang G, Hou J, Shi J, Yu G, Lu B, Zhang X. Soluble CD276 (B7-H3) is released from monocytes, dendritic cells and activated T cells and is detectable in normal human serum. Immunology 2008; 123:538-46; PMID:18194267; http://dx.doi.org/10.1111/j.1365-2567.2007.02723.x

77. Schlecker E, Fiegler N, Arnold A, Altevogt P, Rose-John S, Moldenhauer G, Sucker A, Paschen A, von Strandmann EP, Textor S et al. Metalloprotease-mediated tumor cell shedding of B7-H6, the ligand of the natural killer cell-activating receptor NKp30. Cancer Res 2014; 74:3429-40; PMID:24780758; http://dx.doi.org/10.1158/0008-5472. CAN-13-3017

78. Park JJ, Omiya R, Matsumura Y, Sakoda Y, Kuramasu A, Augustine MM, Yao S, Tsushima F, Narazaki H, Anand S et al. B7-H1/CD80 interaction is required for the induction and maintenance of peripheral T-cell tolerance. Blood 2010; 116:1291-8; PMID:20472828; http:// dx.doi.org/10.1182/blood-2010-01-265975

79. Freeman GJ, Long AJ, Iwai Y, Bourque K, Chernova T, Nishimura H, Fitz LJ, Malenkovich N, Okazaki T, Byrne MC et al. Engagement of the PD-1 immunoinhibitory receptor by a novel B7 family member leads to negative regulation of lymphocyte activation. J Exp Med 2000; 192:1027-34; PMID:11015443; http://dx.doi.org/10.1084/ jem.192.7.1027

80. Nishimura H, Okazaki T, Tanaka Y, Nakatani K, Hara M, Matsumori A, Sasayama S, Mizoguchi A, Hiai H, Minato N et al. Autoimmune dilated cardiomyopathy in PD-1 receptor-deficient mice. Science 2001; 291:319-22; PMID:11209085; http://dx.doi.org/10.1126/science.291.5502.319

81. Jiang Y, Li Y, Zhu B. T-cell exhaustion in the tumor microenvironment. Cell Death Dis 2015; 6:e1792; PMID:26086965; http://dx.doi. org/10.1038/cddis.2015.162

82. Freije JM, Diez-Itza I, Balbin M, Sanchez LM, Blasco R, Tolivia J, Lopez-Otin C. Molecular cloning and expression of collagenase-3, a novel human matrix metalloproteinase produced by breast carcinomas. J Biol Chem 1994; 269:16766-73; PMID:8207000

83. Heredia NJ, Belgrader P, Wang S, Koehler R, Regan J, Cosman AM, Saxonov S, Hindson B, Tanner SC, Brown AS et al. Droplet Digital PCR quantitation of HER2 expression in FFPE breast cancer samples. Methods 2013; 59:S20-3; PMID:23036330; http://dx.doi.org/10.1016/j. ymeth.2012.09.012

84. Hindson BJ, Ness KD, Masquelier DA, Belgrader P, Heredia NJ, Makarewicz AJ, Bright IJ, Lucero MY, Hiddessen AL, Legler TC et al. High-throughput droplet digital PCR system for absolute quantitation of DNA copy number. Anal Chem 2011; 83:8604-10; PMID:22035192; http://dx.doi.org/10.1021/ac202028g